Degenerate Systems of Capacitively-Coupled Josephson Junctions

Sam Kennerly

Ph.D. Qualifying Examination, Drexel University, June 2008
Supervising Professor: Dr. Robert Gilmore
Co-Supervising Professor: Dr. Roberto Ramos

Table of Contents:

0. Abstract

Brian Josephson first predicted the existence of "tunneling supercurrents" between two superconductors at equal voltage in 1962 [1]. A. B. Pippard had considered a similar idea in 1961, but predicted that the probability of both electrons in a Cooper pair simultaneously tunneling was so small as to be unobservable. Pippard's conclusion was supported by many physicists, including BCS theory co-author John Bardeen, but later experimental evidence supported Josephson's prediction [2].

Modern applications of Josephson junctions include voltage standards and high-precision SQUID magnetic-field detectors for use in physics, medicine, geology, and astronomy [4]. Josephson junctions are also of great interest in basic research because they provide testable examples of macroscopic entanglement [25], the Aharanov-Bohm effect [6], and possibly also of Bell's inequality [14]. Capacitively-coupled Josephson junctions in particular show promise as qubit representations for logic gates and/or memory registers in quantum computers [22] [20] [17].

This paper examines systems made from multiple identical junctions coupled by identical capacitors. The behavior of single junctions is developed in detail, and then the possible degeneracies of several multiply-coupled systems are determined from the topology of the systems' circuit diagrams. Each of the first four sections addresses a specific question from Josephson junction theory:

1. Under what conditions can a system be described by Josephson's equations?
Josephson's equations are derived following a method proposed by Richard Feynman in which supercurrent is predicted as the result of phase interference between two weakly coupled quantum systems [3]. The assumptions used in Feynman's derivation are stated as explicitly as possible so that the model may be later expanded to include phenomena such as decoherence or thermal fluctuations.

2. Why is the relative phase coordinate γ not restricted to the range $[0, 2\pi)$?
The RCSJ model of a Josephson junction is presented and a Lagrangian is found for the case $R \rightarrow \infty$. A classical system with an identical Lagrangian (but different numerical constants) is found to possess a phase space that, for some initial conditions, is not topologically compact. It is shown that a "decompactified" phase coordinate γ can be used to describe such a system.

3. Why does the RCSJ junction model appear to produce a classical Hamiltonian?
The equation of motion used to find the RCSJ Hamiltonian specifies a coordinate and its conjugate momentum simultaneously, in violation of the uncertainty principle. This result is shown to be a consequence of applying Kirchhoff's classical laws to quantum operators. A slightly modified method is proposed and an uncertainty relationship is found for junction voltage and supercurrent.

4. Can a system of coupled junctions possess degenerate metastable states?
Systems of two capacitively-coupled junctions are known to exhibit "avoided crossing" behavior in which the excited metastable states of two identical junctions are nondegenerate [25]. An algorithm is found for constructing the Hamiltonian of any system of junctions coupled by capacitors. The symmetries of these Hamiltonians show that degenerate metastable states must be produced for some of these systems.

1. Derivation of Josephson's equations

When two superconductors are separated by a thin insulating barrier, Josephson's equations predict the relationship between voltage across the junction and tunneling supercurrent through the barrier. The simplified explanation of tunneling supercurrent presented here portrays supercurrents as a byproduct of phase interference between two weakly coupled quantum systems [3]. The systems of interest in this paper are superconducting Josephson junctions, but the predicted effects should be observable in any system for which similar assumptions hold. Josephson's equations also accurately describe, for example, two containers of liquid helium connected by an aperture [23].

1.1 Feynman's model

Feynman modelled a Josephson junction as two interacting systems of condensates, each composed of a large number of bosons each with charge $2e$ and mass $2m_e$. The following conditions are assumed:

1. Two subsystems each consist of many bosons simultaneously occupying a single quantum state. These states are labeled Ψ_1 and Ψ_2. The bosons never occupy higher-energy states.

2. Each subsystem, if uncoupled, would be an energy eigenstate. The individual wavefunctions of the uncoupled systems would not evolve in time *except* for time-dependent phase factors ϕ_1, ϕ_2 :
$$\Psi_1(t) = \Psi_1(0)\ e^{\iota\phi_1} \qquad \text{and} \qquad \Psi_2(t) = \Psi_2(0)\ e^{\iota\phi_2}$$

3. The coupling between systems is weak enough that the individual wavefunctions are not significantly altered. The wavefunction for the entire system is a superposition of Ψ_1 and Ψ_2 :
$$\Psi = \alpha\Psi_1 + \beta\Psi_2 \quad \text{where } \alpha, \beta \in \mathbb{C}$$

4. The coupled subsystems can exchange particles. The composite wavefunction remains normalized, but α and β may change. The number density of particles in each subsystem is:
$$n_1 = ||\alpha||^2 \quad n_2 = ||\beta||^2 \quad n_{total} = ||\alpha||^2 + ||\beta||^2 = 1$$

5. Except for their mutual interaction, the subsystems are completely isolated from the environment. With no other interactions present, the composite wavefunction can then be written in the form:
$$\Psi(t) = (\sqrt{n_1}e^{\iota\phi_1})\Psi_1(0) + (\sqrt{n_2}e^{\iota\phi_2})\Psi_2(0)$$
where the variables n_1, n_2, ϕ_1, ϕ_2 are time-dependent.

6. The coupling between the two subsystems is time-independent and symmetric. Specifically,
$$\partial_t \hat{K} = 0 \quad \text{and} \quad \langle\Psi_1|\hat{K}|\Psi_2\rangle = \langle\Psi_2|\hat{K}|\Psi_1\rangle$$
where the operator $\hat{K}$ represents the interaction energy of the coupled subsystems.

Using Ψ_1 and Ψ_2 as a basis, the composite system can be represented by a complex column vector. The Hamiltonian operator in this basis is a 2x2 Hermitian matrix. The Schrödinger equation is:

$$\partial_t \Psi = -\frac{\imath}{\hbar} \hat{H} \Psi \quad \Leftrightarrow \quad \left[\begin{array}{c} \dot{\alpha} \\ \dot{\beta} \end{array} \right] = \frac{-\imath}{\hbar} \left[\begin{array}{cc} E_1 & K \\ K & E_2 \end{array} \right] \left[\begin{array}{c} \alpha \\ \beta \end{array} \right]$$

Here E_1 and E_2 are the ground-state energies of the uncoupled subsystems and K is a constant. Since H is Hermitian, K must be real. The value of K depends on the coupling between the two subsystems.

1.2 Assumptions of Feynman's model

I and II :   At low temperature, BCS theory predicts that electrons in a superconductor can form strongly-correlated pairs called Cooper pairs [4]. In Feynman's derivation, all electrons in a superconductor form Cooper pairs, each pair is modeled as a single boson, and all of these pairs are assumed to occupy the lowest-possible energy eigenstate. The impossibility of cooling any system to absolute zero means that not all Cooper pairs will occupy the lowest possible energy state, but at mK-scale temperature, superconductor electrons (and liquid ^{4}He) are well-approximated this way [4] [23].

III and IV: Assumptions III and IV require that any coupling between the subsystems be "weak, but not too weak." Any coupling strong enough to significantly alter the ground-state wavefunction of either subsystem renders Feynman's model invalid. Conversely, if the coupling energy K is extremely weak, then the model predicts an extremely weak tunneling current. A "too-weak" coupling is one in which the critical supercurrent cannot be detected or is easily overshadowed by noise and external interference.

V: Assumption V is arguably the least realistic assumption of Feynman's model - even under carefully controlled laboratory conditions, no system is ever completely isolated. To accomodate assumption V, Josephson junction experiments are carried out inside a superconducting Faraday cage and at the lowest temperature possible. Even then, the Cooper pairs in each superconductor can interact with the dielectric material, the nuclei of the superconducting material itself, and the atoms in the wires used to connect the circuit to measuring equipment. In practice, interactions ignored by assumption V can interfere with the entanglement of the two superconductor wavefunctions. This phenomenon is known as *decoherence*, and it is both a major challenge to building a working quantum computer [19] and of considerable theoretical interest even outside the field of quantum computing[1].

VI: For a Josephson junction, assumption VI seems self-evident; a dielectric barrier should be equally impenetrable to Cooper pairs from either direction, and the barrier is not significantly altered over the time scales of a junction experiment. But if an asymmetric barrier (perhaps a p-n semiconductor) was present between subsystems, Feynman's model would produce an incorrect Schrödinger equation.

---

[1] Some theorists have suggested that a more detailed understanding of decoherence may help reconcile Erwin Schrödinger's objections to the nonunitary "quantum jumping" in John von Neumann's theory of wavefunction collapse, though this suggestion remains controversial [13] [21].

1.3 Josephson's equations

In their usual form, Josephson's equations rely on one more simplfying assumption:

7.   The subsystems contain a nearly equal number of particles, and the current between subsystems is too small to significantly change the number density in either subsystem: $\sqrt{n_1} \approx \sqrt{n_2}$.

The particle-number-density currents from one system to the other can be written in terms of α and β :

$$\alpha = \sqrt{n_1}e^{\imath\phi_1} \ \Rightarrow \ \dot{\alpha} = \tfrac{1}{2}(n_1)^{-\frac{1}{2}}\dot{n}_1 e^{\imath\phi_1} + \imath \ \dot{\phi}_1 \sqrt{n_1}e^{\imath\phi_1}$$

$$\alpha^*(\dot{\alpha}) = \sqrt{n_1}e^{-\imath\phi_1}\left(\tfrac{1}{2}(n_1)^{-\frac{1}{2}}\dot{n}_1 e^{\imath\phi_1} + \imath\dot{\phi}_1\sqrt{n_1}e^{\imath\phi_1}\right) = \tfrac{1}{2}\dot{n}_1 + \imath\dot{\phi}_1 n_1$$

$$\alpha(\dot{\alpha})^* = (\alpha^*\dot{\alpha})^* = \tfrac{1}{2}\dot{n}_1 - \imath\dot{\phi}_1 n_1$$

$$\alpha^*(\dot{\alpha}) + \alpha(\dot{\alpha})^* = \tfrac{1}{2}\dot{n}_1 + \tfrac{1}{2}\dot{n}_1 = \dot{n}_1$$

$$\dot{n}_1 = \alpha^*(\dot{\alpha}) + \alpha(\dot{\alpha})^* \qquad \dot{n}_2 = \beta^*(\dot{\beta}) + \beta(\dot{\beta})^*$$

By assumptions 4 and 5, total particle number must be conserved. Therefore these currents must be equal in magnitude and opposite in sign. Using this fact and the Schrödinger equation, we find that

$$\imath\hbar \ \dot{n}_1 = E_1||\alpha||^2 + K\alpha^*\beta - E_1||\alpha||^2 - K\alpha\beta^* = K(\alpha^*\beta - \alpha\beta^*)$$

$$\dot{n}_1 = -\imath\frac{K}{\hbar}\sqrt{n_1 n_2}(e^{\imath(\phi_2-\phi_1)} - e^{\imath(\phi_1-\phi_2)})$$

$$\dot{n}_1 = 2\frac{K}{\hbar}\sqrt{n_1 n_2} \ \sin(\phi_2 - \phi_1)$$

Josephson's first equation is a special case of this result. If (nearly) all of the electrons in each superconductor form Cooper pairs with charge -2*e*, then the measured supercurrent I_s in a Josephson junction must be -2*e* times the number of particles crossing into the second subsystem per second :

$$I_s = -2e \ \dot{n}_2 = 2e \ \dot{n}_1 = 4e\frac{K}{\hbar}\sqrt{n_1 n_2} \ \sin(\phi_2 - \phi_1)$$

Using assumption 7, the tunnelling supercurrent I_s in a junction is given by **Josephson's first equation**:

$$I_s = I_0 \sin(\gamma)$$

where *γ* is the phase difference between the subsystems and I_0 is a constant called the **critical current :**

$$\gamma \equiv \phi_2 - \phi_1 \qquad I_0 \equiv 4e\frac{K}{\hbar}n_1 \cdot (\text{volume of subsystem 1})$$

Josephson's second equation relates $\dot{\gamma} = \dot{\phi_2} - \dot{\phi_1}$ to the voltage difference across the junction barrier. Recalling the previous results, we can write $\dot{\phi_1}$ as a function of α :

$$\alpha^*\dot{\alpha} = \tfrac{1}{2}\dot{n} + \imath\dot{\phi_1}n_1 \qquad \alpha(\dot{\alpha})^* = (\alpha^*\dot{\alpha})^* = \tfrac{1}{2}\dot{n} - \imath\dot{\phi_1}n_1$$

$$\imath||\alpha||^2\dot{\phi_1} = \imath n_1\dot{\phi_1} = \tfrac{1}{2}(\alpha^*\dot{\alpha} - \alpha(\dot{\alpha})^*) \quad \Rightarrow \quad \dot{\phi_1} = \tfrac{-\imath}{2||\alpha||^2}(\alpha^*\dot{\alpha} - \alpha(\dot{\alpha})^*)$$

A similar equation in terms of *β* can be found for $\dot{\phi_2}$. Using the Schrödinger equation, we find :

$$\dot{\alpha} = \frac{-\imath}{\hbar}(E_1\alpha + K\beta) \qquad \dot{\beta} = \frac{-\imath}{\hbar}(K\alpha + E_2\beta)$$

$$\dot{\phi_1} = \frac{-\imath}{2\hbar||\alpha||^2}(\alpha^*(-\imath E_1\alpha - \imath K\beta) - \alpha(\imath E_1\alpha^* + \imath K\beta^*))$$

$$\hbar\,\dot{\phi_1} = -E_1 - \frac{1}{2||\alpha||^2}K(\alpha^*\beta + \alpha\beta^*)$$

$$\hbar\dot{\phi_1} = -E_1 - \frac{1}{2n_1}K\sqrt{n_1 n_2}(e^{\imath(\phi_2-\phi_1)} + e^{\imath(\phi_1-\phi_2)})$$

$$\hbar\,\dot{\phi_1} = -E_1 - K\frac{\sqrt{n_1 n_2}}{n_1}\cos(\gamma)$$

A result for $\dot{\phi_2}$ is found in the same way, but with *E₂* in place of *E₁* . Using assumption 7 again,

$$\hbar\,\dot{\gamma} = -E_2 - K\cos(\gamma) + E_1 + K\cos(\gamma) = E_1 - E_2$$

The energy difference between subsystems can be measured indirectly by connecting a voltmeter across the junction barrier. If the voltmeter reads *V* , then each Cooper pair "sees" an energy difference *qV* :

$$qV = -2eV = E_2 - E_1$$

The result is **Josephson's second equation**, shown here with the definition of the **flux quantum** Φ_0 :

$$V = \frac{\Phi_0}{2\pi}\,\dot{\gamma} \qquad \Phi_0 \equiv \frac{h}{2e}$$

2. The washboard potential

Consider a Josephson junction with one end connected to a current supply and the other end to a grounded object with an ample supply of free electrons. Current can pass through the junction via three possible channels [5]:

Channel R: Conduct conventionally through the dielectric barrier, which then acts a resistor.
Channel C: Accumulate a charge difference on either side of the barrier, which then acts as a capacitor.
Channel X: Tunnel through the barrier as a supercurrent.

The resulting system is thus often modeled as a resistor-capacitor-shunted-junction (RCSJ) diagram, as shown to the right. I_b is the external current source (called a *bias current*), R is the resistivity of the barrier, and C_J is the capacitance of the barrier. The X in the center represents the junction itself. If the barrier is a strong enough insulator, then negligbly few electrons will conduct conventionally and $R \to \infty$. In this case, the R channel can be ignored.
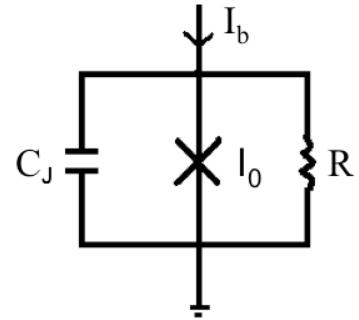
A quantum-mechanical description of the RCSJ model can be formed by the following procedure [14] [17]:

1. Use Josephson's equations to write the current and voltage across the X in terms of γ and $\dot{\gamma}$.
2. Use Kirchhoff's (classical) laws of current conservation and voltage to write an equation of motion.
3. Choose a Lagrangian $\mathcal{L}$ consistent with the equation of motion in step 2.
4. Find the momentum $\mathbb{P}$ conjugate to γ and Legendre transform $\mathcal{L}$ to find a Hamiltonian $\mathcal{H}$.
5. Define a quantum operator p according to the canonical quantum-mechanical relationships:
$$p \equiv -i\hbar\partial_\gamma \qquad [\gamma, p] = i\hbar$$
6. Form a quantum Hamiltonian H by substituting the p operator for $\mathbb{P}$ into the classical Hamiltonian $\mathcal{H}$.

The next subsection covers steps 1-4. A brief detour is made to consider a classical system with identical Lagrangian, Hamiltonian, and equation of motion, then steps 5-6 are covered in section 3.

2.1 Single-junction Lagrangian and Hamiltonian for the case $R \to \infty$

This paper considers only junctions in which conventional conductivity is negligible. Kirchhoff's laws then tell us that 1) current through the C channel plus current through the X channel must equal the bias current, and 2) voltage drop is the same across both channels. For an ideal classical capacitor,

$$C_J \equiv \frac{Q}{V} \quad \Rightarrow \quad I_C = \dot{Q} = C_J \dot{V}$$

Combining these expressions with both of Josephson's equations gives the following current equation:

$$I_b = I_s + I_c = I_0 \sin(\gamma) + C_J \left(\frac{\Phi_0}{2\pi}\right) \ddot{\gamma}$$

Now that an equation of motion is known, the goal is to find a Lagrangian consistent with this equation. Here we simply state such a Lagrangian and check that it is consistent with the Euler-Lagrange condition. (Some motivation for this choice of Lagrangian is given later in the section on mechanical analogies.)

$$\mathcal{L} = \left(\frac{\Phi_0}{2\pi}\right) \left[\frac{1}{2} C_J \left(\frac{\Phi_0}{2\pi}\right) (\dot{\gamma})^2 + I_0 \cos(\gamma) + I_b \gamma \right]$$

The flux quantum before the square brackets is not necessary to satisfy the Euler-Lagrange condition, but it does ensure that the Lagrangian has units of energy. Checking for consistency, we find:

$$\frac{\partial \mathcal{L}}{\partial \gamma} = \left(\frac{\Phi_0}{2\pi}\right) \left[-I_0 \sin(\gamma) + I_b\right] \qquad \frac{d}{dt}\left(\frac{\partial \mathcal{L}}{\partial \dot{\gamma}}\right) = \left(\frac{\Phi_0}{2\pi}\right)^2 C_J \ddot{\gamma}$$

$$\frac{d}{dt}\left(\frac{\partial \mathcal{L}}{\partial \dot{\gamma}}\right) = \frac{\partial \mathcal{L}}{\partial \gamma} \qquad \Leftrightarrow \qquad C_J \left(\frac{\Phi_0}{2\pi}\right) \ddot{\gamma} = -I_0 \sin(\gamma) + I_b$$

Our chosen Lagrangian produces the correct equation of motion, and its canonical momentum p is:

$$\mathfrak{p} \equiv \frac{\partial \mathcal{L}}{\partial \dot{\gamma}} = \left(\frac{\Phi_0}{2\pi}\right)^2 C_J \ \dot{\gamma}$$

We now perform a Legendre transformation on the Lagrangian to obtain a Hamiltonian:

$$\mathcal{H} \equiv \dot{\gamma}\mathfrak{p} - \mathcal{L} = \left(\frac{\Phi_0}{2\pi}\right) \left[\frac{1}{2} C_J \left(\frac{\Phi_0}{2\pi}\right) (\dot{\gamma})^2 - I_0 \cos(\gamma) - I_b \gamma \right]$$
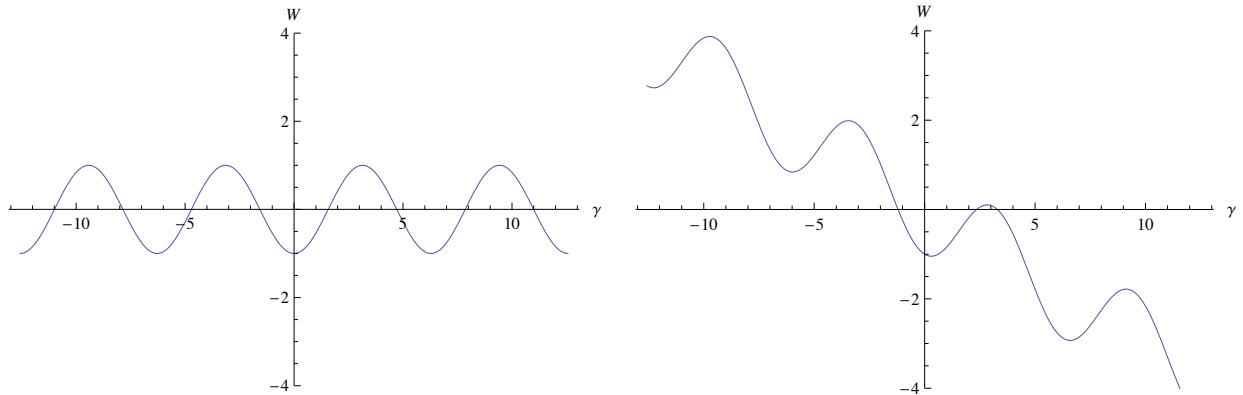
To simplify the notation, define two functions T and W in the following way:

$$T \equiv \frac{1}{2} C_J \left(\frac{\Phi_0}{2\pi}\right)^2 (\dot{\gamma})^2 \qquad W \equiv -\left(\frac{\Phi_0}{2\pi}\right) \left[I_0 \cos(\gamma) + I_b \gamma \right]$$

Using these functions, the Lagrangian and Hamiltonian can be written in a more familiar form:

$$\mathcal{L} = T - W \qquad \mathcal{H} = T + W$$

The function W so defined is called the **washboard potential**. Two examples are plotted below:

Washboard potentials for I_b/I_0 = 0 and 0.3 . Y-axis scale is 1 = $\left(\frac{\Phi_0}{2\pi}\right) I_0$ and x-axis is dimensionless.

Using Josephson's second equation, the function *T* equals the classical energy formula for a capacitor:

$$\tfrac{1}{2}C_J V^2 = \tfrac{1}{2}C_J \left(\tfrac{\Phi_0}{2\pi}\right)^2 (\dot{\gamma})^2$$

This equality provides some justification for the overall factor of the flux quantum in the Lagrangian.

2.2 Mechanical analogy to the RCSJ equations of motion

Some useful insight into the dynamics of Josephson junctions can be gained by considering a classical system with a similar Lagrangian. The following example is described in [4 p109]:

Imagine a mass *m* attached to one end a rigid, massless rod of length *r*. If the other end of the rod is attached to a fixed point but allowed to rotate, the result is a pendulum with a 360⁰ range of motion. Orient the pendulum so that its axis is exactly horizontal, and define γ to be the angle between the rod and the direction of gravity **g** so that γ = 0 when the rod is at its lowest point. If the pendulum is subjected to a constant torque Γ, then the resulting equation of motion from Newtonian mechanics is:

$$mr^2\ddot{\gamma} + mgr(\sin\gamma) = \Gamma$$

This Lagrangian for this system follows from the classical expressions for kinetic and potential energy:

$$\mathcal{L} \;=\; \tfrac{1}{2}mr^2(\dot{\gamma})^2 \;+\; mgr\,(\cos\gamma) \;+\; \Gamma\gamma$$

The first two terms are recognizable as rotational kinetic energy and gravitational potential. The last term is an "extra" potential that leads to a constant torque in the equation of motion. This Lagrangian is identical to the one obtained for a Josephson junction with the following subsitutions:

$$C_J \leftrightarrow \frac{1}{m} \qquad \left(\frac{\Phi_0}{2\pi}\right) \leftrightarrow mr \qquad I_0 \leftrightarrow g \qquad I_b \leftrightarrow \frac{\Gamma}{mr} = \frac{F}{m}$$

With these substitutions, the Hamiltonian for the 360⁰ pendulum is also identical to the RCSJ Hamiltonian. (For a junction with nonzero resistivity R, the analogy can be further extended by including a dissipative frictional torque proportional to angular velocity.) Of course, gravitational potential is only defined relative to some reference height: in this case, it is zero for any half-integer value of γ.

Some peculiar features of the quantum-mechanical Josephson junction are also found in the classical 360⁰ pendulum. In particular, advancing the value of γ by a multiple of 2π changes the value of the Lagrangian if the applied torque Γ is nonzero! With no torque, the washboard potential is symmetric under a translation $\gamma \to \gamma + 2\pi$, but the addition of Γ to the system breaks this symmetry. It becomes necessary to use a "decompactified" phase coordinate γ which is *not* restricted to the interval $\lfloor 0, 2\pi)$.

A related property common to the RCSJ model and the 360⁰ pendulum is the existence of bound and unbound states[2]. Depending upon the magnitude of Γ and the initial conditions of γ and $\dot{\gamma}$, the pendulum may oscillate back and forth within a limited range, spin in one direction and then reverse its rotation, or spin in the same direction faster and faster indefinitely. To see this, consider case that applied torque Γ is zero. The pendulum has maximal (positive) gravitational potential energy at top dead center ($\gamma = \pi$). If the pendulum reaches this point with nonzero kinetic energy, its total energy H is sufficient to cause the pendulum to rotate indefinitely. If the pendulum cannot reach top dead center, it will never have enough total energy H to do so. In particular, if at any time the Hamiltonian returns a number $h > mgr$, then the Hamiltonian must always do so and the pendulum will be "unbound." If the inequality is reversed, the pendulum remains permanently "bound." (If the terms are equal, the pendulum is neutrally stable at top dead center; any perturbation whatsoever will lead to a bound or unbound state.)

Because the Lagrangian of this system does not explicitly depend on *t*, the value returned by the Hamiltonian must be constant in time [18 p62]. For nonzero torque Γ, the Hamiltonian is:

$$\mathcal{H} = T + W = \tfrac{1}{2}mr^2(\dot{\gamma})^2 - mgr\left(\cos\gamma\right) - \Gamma\gamma$$

When a torque Γ is applied, it is useful to separate the Hamiltonian into two parts: a "system energy" term consisting of kinetic + gravitational energy, minus an "applied energy" term $\Gamma\gamma$:

$$E(t) \equiv \tfrac{1}{2}mr^2(\dot{\gamma})^2 - mgr(\cos\gamma) \qquad \mathcal{H} = E(t) - \Gamma\gamma$$

The system energy *E*(t) is *not* conserved, but the overall value of *H* is constant in time. Numerical solutions to the equations of motion and energy equation are shown here as functions of time:

---

[2] As explained later, the quantum RCSJ model does not allow the existence of truly bound states, but long-lived resonances called *metastable states* can exist. The analogy is still useful, however!

Case 1 Bound pendulum: $E(0) < mgr$ and $|\Gamma|$ is small. The pendulum oscillates, but never reaches the top of its path $\gamma = \pi$. These solutions are periodic (but not necessarily sinusoidal).
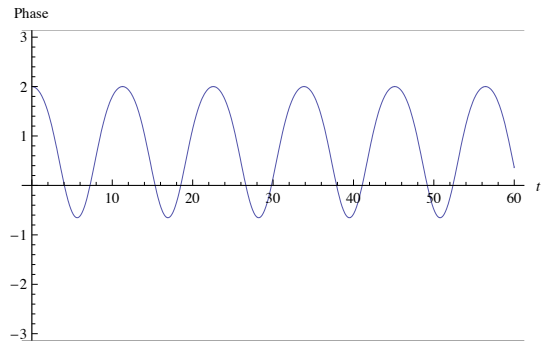
Case 2 Bound pendulum becomes unbound: $E(0) < mgr$, but $|\Gamma|$ is large. The applied torque is eventually sufficient to push the pendulum "over the top," after which point it continues to spin in the same direction indefinitely and γ increases without bound. The horizontal line marks "top dead center," $\gamma = \pi$.
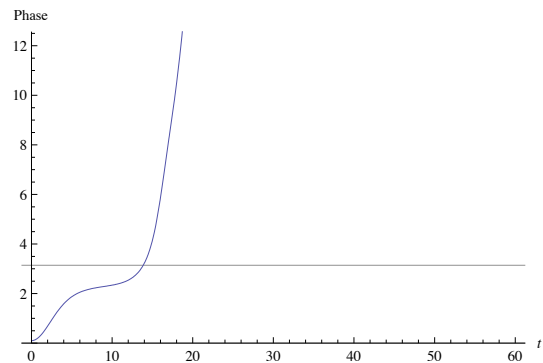
Case 3 Reflected unbound pendulum: $E(0) > mgr$, but Γ is applied in the direction opposite the pendulum's initial velocity. The pendulum passes $\gamma = -\pi$, but its direction of rotation is eventually reversed by the applied torque. The pendulum inevitably "escapes" past $\gamma = +\pi$, and then γ increases without bound.
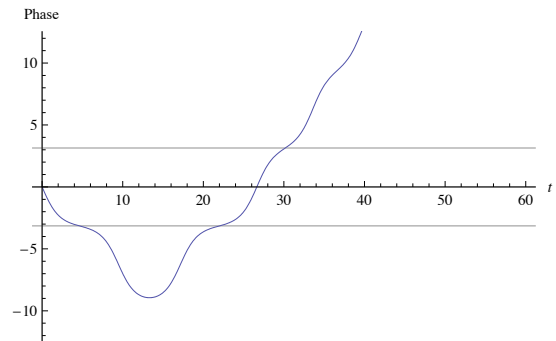
Case 4 Unbound pendulum remains unbound: $E(0) > mgr$ and Γ is in the direction of initial velocity. The pendulum quickly goes "over the top" and γ increases without bound.
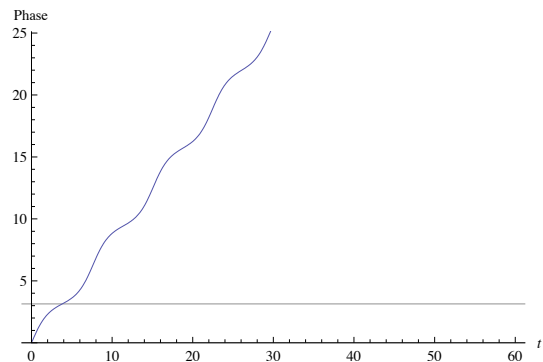
Driving a pendulum "over the top" bears a striking correspondence to a *switching event,* in which the voltage V across a current-biased junction switches from zero to a finite value. In an overdriven pendulum, the average value of $\dot{\gamma}$ also switches from zero to a steadily increasing (or decreasing) value. Josephson's second equation shows that V is proportional to $\dot{\gamma}$, so the analogy is quite close!

2.3 Decompactification of the phase coordinate γ

Both the 360^0 pendulum Hamiltonian and the quantum-mechanical Hamiltonian used to describe a Josephson junction are written in terms of a phase coordinate γ that is *not* restricted to a closed, compact domain [22]. It is interesting that this "decompactification" of γ is a shared feature of the classical and quantum systems: in either system, increasing γ by 2π changes the value of the Hamiltonian. While some proposed explanations for decompactification consider it a result of some unspecified quantum-mechanical interaction with a junction's environment, these explanations may be unnecessary[3]. The phase space for a purely classical, completely isolated 360^0 pendulum is noncompact; perhaps the quantum Hamiltonian inherits this feature from its classical counterpart.

In the case of the 360^0 pendulum, it is not physically realistic to assume that one periodic coordinate $\gamma(t) \in [0, 2\pi)$ can describe the system for all *t*. Complete information about the system at time *t* requires two initial conditions, the value of γ, *and* the number of rotations made by the pendulum since *t* = 0. More precisely, note that the state of the pendulum at any time can be completely described by an ordered pair $(\gamma(t), \dot{\gamma}(t))$. Any possible time-evolution of the system can then be described by a parametrized trajectory $(\gamma, \dot{\gamma})$. The phase space of the classical 360^0 pendulum consists of all possible points through which such a trajectory could pass. If the initial conditions lead to unbound solutions, then the possible values of $\dot{\gamma}$ cover an interval $[min(\gamma), \infty)$. If the possible values of γ cover the circle S^1, then $(\gamma, \dot{\gamma})$ can pass through any point on the half-cylinder $S_1 \times [min(\gamma), \infty)$. The classical phase space of this system is not compact: trajectories $(\gamma, \dot{\gamma})$ for unbound solutions can spiral around the half-cylinder with ever-increasing (or decreasing) values of $\dot{\gamma}$ as *t* increases. Thus it is not entirely suprising that a "decompactified" parameter must be used to completely describe the system in question.

3. Quantum mechanics of a driven Josephson junction

When forming a quantum-mechanical description of the RCSJ model, we are faced with an apparent paradox: the equation of motion (and the Lagrangian and Hamiltonian) obtained from Josephson's equations and Kirchhoff's laws is an equation of *coordinates*, not *operators*. The phase coordinate γ and its conjugate momentum ℘ are both specified simultaneously in the Hamiltonian of the system, and the resulting system is completely deterministic given two appropriate initial conditions. But in a quantum-mechanical system, simultaneously specifying a coordinate and its conjugate momentum violates the uncertainty principle! This apparent paradox can be avoided with one more assumption:

8. Kirchhoff's laws apply only to the *expectation values* $\langle V \rangle$ and $\langle I \rangle$ of the quantum operators $\hat{V}$ and $\hat{I}$. An ideal capacitor obeys the classical law $\langle Q \rangle = C \langle V \rangle$ where capacitance *C* is a constant.

Using assumption 8, Kirchhoff's laws can be written in terms of expectiation values:

---

[3] Environmental interactions may still be necessary to explain the source of decoherence*.*

$$\langle I_b \rangle = \langle I_s \rangle + \frac{d}{dt}\langle Q \rangle = \langle I_s \rangle + C_J \frac{d}{dt}\langle V \rangle$$

where we have used the (classical) ideal capacitor law $\langle Q \rangle = C\langle V \rangle$. Josephson's equations then require:

$$\langle I_s \rangle = I_0 \langle \sin(\gamma) \rangle \qquad \langle V \rangle = \left(\frac{\Phi_0}{2\pi}\right)\langle \dot{\gamma} \rangle$$

$$\langle I_b \rangle = I_0 \langle \sin(\gamma) \rangle + C_J \left(\frac{\Phi_0}{2\pi}\right)\frac{d}{dt}\langle \dot{\gamma} \rangle$$

3.1 Quantum Hamiltonian with washboard potential

We now wish to find operators $\hat{H}$ and $\hat{p}$ which predict this relationship between expectation values. Recall that the Hamiltonian and canonical momentum suggested for the RCSJ model were:

$$\mathcal{H} \equiv \dot{\gamma}\mathfrak{p} - \mathfrak{L} = \left(\frac{\Phi_0}{2\pi}\right)\left[\frac{1}{2}C_J\left(\frac{\Phi_0}{2\pi}\right)(\dot{\gamma})^2 - I_0 \cos(\gamma) - I_b\gamma\right]$$

$$\mathfrak{p} \equiv \frac{\partial \mathfrak{L}}{\partial \dot{\gamma}} = \left(\frac{\Phi_0}{2\pi}\right)^2 C_J \, \dot{\gamma}$$

$$\mathcal{H} = \left(\frac{\Phi_0}{2\pi}\right)^{-2}\frac{1}{2C_J}\mathfrak{p}^2 - \left(\frac{\Phi_0}{2\pi}\right)I_0 \cos(\gamma) - \left(\frac{\Phi_0}{2\pi}\right)I_b\gamma$$

Using Josephson's second equation, define an operator $\hat{p}$ to replace the coordinate $\mathfrak{p}$ in this way:

$$\hat{p} \equiv \left(\frac{\Phi_0}{2\pi}\right)C_J\hat{V} = \left(\frac{\Phi_0}{2\pi}\right)^2 C_J \frac{d}{dt}\hat{\gamma}$$

Posit that $\hat{p}$ obeys the familiar quantum-mechanical rules for a momentum operator conjugate to $\hat{\gamma}$:

$$\hat{\gamma}\Psi(\gamma) = \gamma\Psi(\gamma) \qquad \hat{p}\Psi(\gamma) = -\imath\hbar\partial_\gamma\Psi(\gamma) \qquad [\hat{\gamma}, \hat{p}] = \imath\hbar$$

Now substitute the operators $\hat{p}$ and $\hat{\gamma}$ for their classical counterparts in the previous Hamiltonian:

$$\hat{H}\Psi = \frac{-\hbar^2}{2C_J}\left(\frac{\Phi_0}{2\pi}\right)^{-2}\partial_\gamma^2\Psi - \left(\frac{\Phi_0}{2\pi}\right)I_0 \cos(\gamma)\Psi - \left(\frac{\Phi_0}{2\pi}\right)I_b\gamma\Psi$$

Rewrite this in a more familiar form by defining a "moment of inertia" μ and a washboard potential $\hat{W}$:

$$\mu \equiv C_J\left(\frac{\Phi_0}{2\pi}\right)^2 \qquad \hat{W} \equiv \left(\frac{\Phi_0}{2\pi}\right)(-I_0 \cos(\gamma) - I_b\gamma) \qquad \hat{H}\Psi = \frac{\hat{p}^2}{2\mu}\Psi + \hat{W}\Psi$$

Heisenberg's equation of motion gives the desired rules for time evolution of expectation values:

$$\frac{d}{dt}\langle p\rangle = \frac{\imath}{\hbar}\langle[\hat{H},\hat{p}]\rangle \qquad \frac{d}{dt}\langle\gamma\rangle = \frac{\imath}{\hbar}\langle[\hat{H},\hat{\gamma}]\rangle$$

Since any operator commutes with its own square, we need only find the commutator $[\hat{W},\hat{p}]$:

$$[\hat{W},\hat{p}]\Psi = \hat{W}\hat{p}\Psi - \hat{p}\hat{W}\Psi = -\imath\hbar\hat{W}(\partial_\gamma\Psi) + \imath\hbar\partial_\gamma(\hat{W}\Psi)$$

$$= \imath\hbar\left(\frac{\Phi_0}{2\pi}\right)\left(I_0\cos(\gamma)\left(\partial_\gamma\Psi\right) + I_b\gamma\left(\partial_\gamma\Psi\right) - \partial_\gamma\left(I_0\cos(\gamma)\Psi + I_b\gamma\Psi\right)\right)$$

The last term can be expanded using the product rule and re-inserted into the previous expression:

$$\partial_\gamma\left(I_0\cos(\gamma)\Psi + I_b\gamma\Psi\right) = -I_0\sin(\gamma)\Psi + I_0(\cos(\gamma))\left(\partial_\gamma\Psi\right) + I_b\Psi + I_b\gamma\left(\partial_\gamma\Psi\right)$$

$$[\hat{W},\hat{p}] = \imath\hbar\left(\frac{\Phi_0}{2\pi}\right)\left(I_0\sin(\gamma) - I_b\right)$$

Using the Heisenberg's first equation gives the following equation of motion for $\langle\hat{p}\rangle$:

$$\frac{d}{dt}\langle p\rangle = \left(\frac{\Phi_0}{2\pi}\right)\left(-I_0\langle\sin(\gamma)\rangle + \langle I_b\rangle\right) = \left(\frac{\Phi_0}{2\pi}\right)\left(-\langle I_s\rangle + \langle I_b\rangle\right)$$

where the right side has been rewritten using Josephson's first equation. Recalling the definition of $\hat{p}$,

$$C_J\frac{d}{dt}\langle V\rangle + \langle I_s\rangle = \langle I_b\rangle$$

This is the same result found by combining Kirchhoff's conservation equation with Josephson's first equation, but with both written in terms of expectation values. The second Heisenberg equation gives:

$$\frac{d}{dt}\langle\gamma\rangle = \frac{\imath}{\hbar}\langle[\hat{H},\hat{\gamma}]\rangle = \frac{\imath}{\hbar\mu}\langle[\hat{p}^2,\hat{\gamma}]\rangle$$

since $\hat{\gamma}$ commutes with itself and powers of itself and $\cos(\hat{\gamma})$ can be written as powers of $\hat{\gamma}$. Using the canonical commutation relationship $[\hat{\gamma},\hat{p}] = \imath\hbar$, it can be shown that $[\hat{p}^2,\hat{\gamma}] = -2\imath\hbar\hat{p}$ and thus,

$$\frac{d}{dt}\langle\gamma\rangle = \frac{\imath}{\hbar\mu}\langle-2\imath\hbar\hat{p}\rangle = \frac{1}{\mu}\langle\hat{p}\rangle = \left(\frac{\Phi_0}{2\pi}\right)^{-1}\langle\hat{V}\rangle$$

which is Josephson's second equation written in terms of expectation values.

3.2 Uncertainty relationship for supercurrent and voltage

Recall that the method described at the beginning of section 2 consists of the following steps:

1. Use Josephson's equations to write the current and voltage across the X in terms of γ and $\dot{\gamma}$.
2. Use Kirchhoff's (classical) laws of current conservation and voltage to write an equation of motion.
3. Choose a Lagrangian $\mathfrak{L}$ consistent with the equation of motion in step 2.
4. Find the momentum $\mathfrak{p}$ conjugate to γ and Legendre transform $\mathfrak{L}$ to find a Hamiltonian $\mathcal{H}$.
5. Define a quantum operator p according to the canonical quantum-mechanical relationships:
$$p \equiv -\imath\hbar\partial_\gamma \qquad [\gamma, p] = \imath\hbar$$
6. Form a quantum Hamiltonian H by substituting the p operator for $\mathfrak{p}$ into the classical Hamiltonian $\mathcal{H}$.

This method produces results consistent with Josephson's equations and Kirchhoff's laws, but it suffers from the paradox mentioned at the beginning of the section: Josephson's equations à la Feynman are obtained using quantum mechanics, but the Hamiltonian in step 4 is classical! Steps 5 and 6 are referred to as "re-quantizing" the system, and it is reasonable to wonder why these steps are necessary [17].

The paradox can be resolved by assuming that the junction voltage and supercurrent in Josephson's equations represent operators $\hat{V}$ and $\hat{I}$, not classical variables $\langle V \rangle$ and $\langle I \rangle$. If so, then it is incorrect to treat γ and $\dot{\gamma}$ as classical phase-space coordinates in steps 2-4. By doing so, the above method inadvertantly "un-quantizes" Josephson's equations to produce a classical Lagrangian and Hamiltonian. When "re-quantized" via steps 5 and 6, however, the resulting quantum Hamiltonian and conjugate momentum operators do predict expectation values consistent with classical circuit theory and behavior consistent with experimental observations (e.g. [14] [15] [19] [25]). Perhaps it is most accurate, then, to view the above method as simply a mnemonic for writing the correct quantum operators.

The operators $\hat{V}$ and $\hat{I}$ in Josephson's equations need not commute [22]. Their commutator is:

$$[\ \hat{V}, \hat{I}_s\ ] = \left(\tfrac{\Phi_0}{2\pi}\right)\mu^{-1}I_0\ [\ -\imath\hbar\partial_\gamma, \sin(\gamma)\ ] = -\imath\hbar(\tfrac{\Phi_0}{2\pi})\mu^{-1}I_0\cos(\gamma)$$

The uncertainties of $\hat{V}$ and $\hat{I}$ must then be related by the generalized uncertainty principle:

$$\Delta_V^2\ \Delta_{I_s}^2 \geq \left(\tfrac{1}{2\imath}\langle[\hat{V}, \hat{I}_s]\rangle\right)^2 = \tfrac{1}{4}\hbar^2\left(\left(\tfrac{\Phi_0}{2\pi}\right)\mu^{-1}I_0\right)^2\langle\cos(\gamma)\rangle^2$$

$$\Delta_V\Delta_{I_s} \geq \tfrac{1}{2}\hbar\left(\tfrac{\Phi_0}{2\pi}\right)\mu^{-1}I_0|\langle\cos(\gamma)\rangle|$$

Order-of-magnitude data from quantum computing experiments [19] [25] leads to an uncertainty of:

$$C_J \approx 1\ \mathrm{pF} \qquad I_0 \approx 10\ \mu A \quad \Rightarrow \quad \tfrac{1}{2}\hbar\left(\tfrac{\Phi_0}{2\pi}\right)\mu^{-1}I_0 \approx 3\cdot 10^{-12}\ \mathrm{watt}$$

Note that this uncertainty relationship relates junction voltage and *supercurrent*, not bias current. If an experiment can be constructed in which supercurrent and junction voltage are both measured directly, then their uncertainties should be related. A junction in a strongly-bound metastable state such that γ remains close to 0 would likely be desirable, as these states maximize the value of $|\langle \cos(\gamma) \rangle|$.

3.3 Metastable states of the washboard potential

Considered as a potential energy function, the washboard potential has no absolute maximum or minimum when the bias current term is nonzero[4]. The washboard does posess *local* minima, but only when $I_b \leq I_0$. The location of a classical particle with such a potential can be bound between two maxima if its energy is low enough, but a quantum particle can possibly tunnel to a lower-energy state. Consequently the Hamiltonian in subsection 3.1 does not permit the existence of energy eigenstates. This feature is obviously not shared by the classical 360^0 pendulum, but it does provide some intuition: a *quantum* pendulum can be located in a superposition of angles γ, some of which are located "over the top." Just as a particle can tunnel through a classically forbidden (finite) barrier, an unsupervised quantum pendulum can tunnel through its gravitational energy barrier *mgr* to become unbound.

If bias current is not too large, the quantum washboard potential does permit the existence of long-lived scattering resonances called metastable states. (Because the transmission probability for a particle in a washboard potential is zero, these states are more accurately described as reflection resonances [16].) A precise definition of *metastable* can be made using the uncertainty principle [7]:

$$\Delta_E \Delta_t \geq \tfrac{1}{2}\hbar \qquad \Delta_t \equiv \Delta_A \left| \tfrac{d}{dt}\langle A \rangle \right|^{-1} \qquad \Rightarrow \qquad \left| \tfrac{d}{dt}\langle A \rangle \right| \leq \tfrac{2}{\hbar}(\Delta_E \Delta_A)$$

where $\hat{A}$ is *any* operator that does not depend *explicitly* on time, and Δ_A is its uncertainty. Thus for a given time scale, if Δ_E is small enough, the rate of change of any expectation value can become negligible. If Δ_E for a state is small enough that every observable $\langle A \rangle$ relevant to a given experiment on a given time scale changes negligibly, that state is said to be metastable. In Josephson junction experiments, the relevant behavior (phase entanglement) is nearly always destroyed by decoherence within ~ 10 ns. Over this time scale, metastable states have been detected experimentally [17].

Finding the wavefunctions and/or energy (expectation) values for washboard resonances can be quite difficult; in the position representation, one must solve a second-order nonlinear differential equation. A number of approximation strategies have been developed, including the following:

1. Approximate the washboard near a local minimum as a quadratic [14] or cubic [17].
2. Impose "rigid-wall" boundary conditions at local maxima and solve numerically [20].
3. Transform the washboard potential via complex rescaling [17].
4. Construct a transfer matrix and match boundary conditions [16].

---

[4] For zero bias current, the washboard is periodic. Such potentials are studied in, for example, [8].

Results from the second method are shown below. The wavefunction of a metastable state is assumed to be zero outside two adjacent maxima of the washboard, and the potential values are calculated on a grid of 1000 steps. The second-derivative operator is replaced by a finite-difference operator:

$$\partial_\gamma^2 \Psi(\gamma) \approx \tfrac{1}{\delta^2}\left[\Psi(\gamma-\delta) - 2\Psi(\gamma) + \Psi(\gamma+\delta)\right]$$

The Hamiltonian is then represented by a 1000 x 1000 matrix which is diagonalized using a numerical routine. For the graph below, the following numerical values from [25] were used:

$$C_J \approx 4.8 \text{ pF} \qquad I_0 \approx 14.779 \ \mu\text{A} \qquad I_b \approx 14.630 \ \mu\text{A} \approx 0.99 \ I_0$$

Ground state and two excited states are shown along with the washboard potential (black line). Y-axis scale for the washboard potential is joules and for the wavefunctions is arbitrary. γ runs along the x-axis.

"Hard-wall" condition $\Psi = 0$ is imposed on all points outside $\gamma \in (1.18, 1.713)$.

Binding energies (energy minus potential energy at right maximum):

ground: -7.96 10^{-24}
1st: -5.37 10^{-24}
2nd: -2.94 10^{-24}
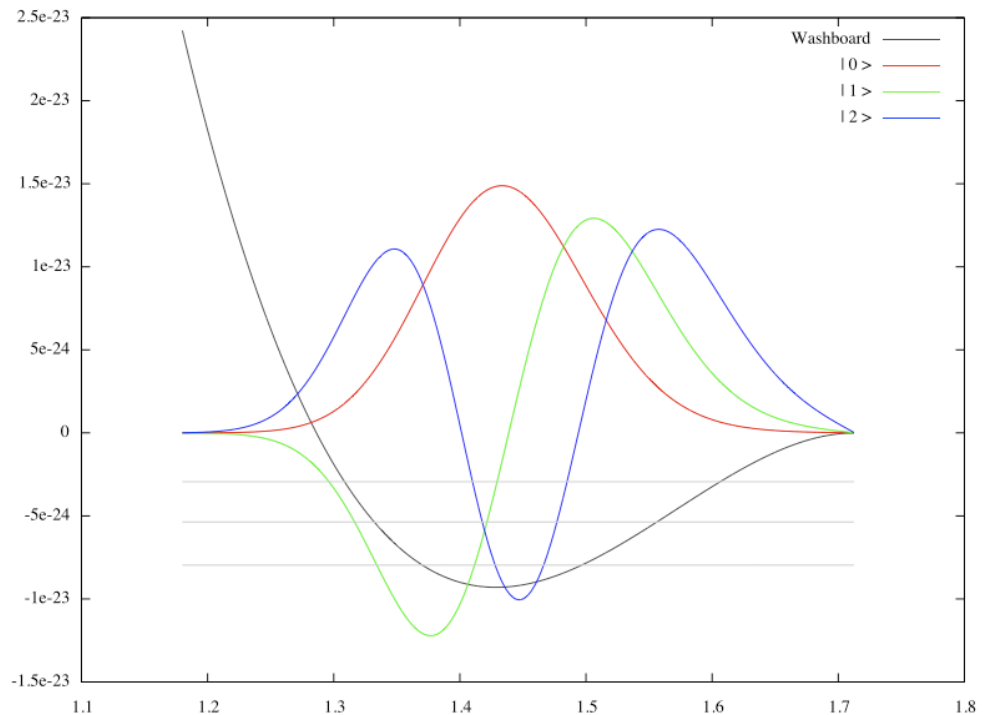
The hard-wall boundary conditions prevent tunneling or scattering, thus solutions produced using this method are always bound states. As would be expected, the wavefunctions and energies obtained tend to be reasonably accurate for long-lived "almost-bound" resonances but quite useless for other purposes. Fortunately, it is these "almost-bound" states that are of interest in Josephson junction spectroscopy. Unfortunately, all of these techniques (except perhaps the quadratic approximation) are computuationally difficult to extend to multiple-junction systems in which the Hamiltonian contains a multidimensional washboard potential. These systems are the subject of the next section.

4. Systems of capacitively-coupled Josephson junctions

Many quantum computing experiments (e.g. [15][19]) focus on the properties of two approximately identical Josephson junctions connected by a conventional capacitor. The metastable states of such a system are entanglements of the single-junction metastable states, which makes capacitively-coupled junctions potentially useful as elements of a quantum computer circuit [17][20][22].

4.1 Two identical junctions connected by a capacitor

The circuit diagram for such a system is shown to the right. Each junction is represented by the RCSJ model with $R \to \infty$ and two independently controlled bias currents are run through the junctions. There are now two phase coordinate operators $\hat{\gamma}_1$ and $\hat{\gamma}_2$ for the system and two conjugate momentum operators. Correct Hamiltonian and conjugate momentum operators for this system must produce expectation values in agreement with Kirchhoff's laws:
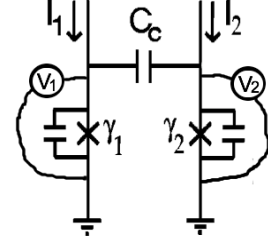
$$\langle I_1 \rangle = \langle I_{s1} \rangle + C_J \frac{d}{dt}\langle V_1 \rangle - C_c \frac{d}{dt}\langle V_2 - V_1 \rangle$$

$$\langle I_2 \rangle = \langle I_{s2} \rangle + C_J \frac{d}{dt}\langle V_2 \rangle + C_c \frac{d}{dt}\langle V_2 - V_1 \rangle$$

Following the method outlined in section 2, a (classical) equation of motion can be found for this system, followed by a Lagrangian, canonical momentum, and Hamiltonian. There is, however, an easier way to obtain an equivalent Hamiltonian. Recall that the $\hat{T}$ term in the single-junction Hamiltonian is equivalent to the classical energy of a capacitor with the $\hat{V}$ operator in place of classical voltage:

$$\tfrac{1}{2}\mu^{-1}\hat{p}^2 = \tfrac{1}{2}\left(C_J\left(\tfrac{\Phi_0}{2\pi}\right)^2\right)^{-1}\left(C_J\left(\tfrac{\Phi_0}{2\pi}\right)\hat{V}\right)^2 = \tfrac{1}{2}C_J\hat{V}^2$$

To find a Hamiltonian for the two-junction system, define a coupling voltage operator $\hat{V}_2 - \hat{V}_1$ and add a coupling energy term $\tfrac{1}{2}C_c(\hat{V}_2 - \hat{V}_1)^2$ to $\hat{H}$ to produce the following (quantum) Hamiltonian:

$$\hat{H}\Psi = \tfrac{1}{2}C_J\hat{V}_1^2\Psi + \tfrac{1}{2}C_J\hat{V}_1^2\Psi + \tfrac{1}{2}C_C(\hat{V}_2 - \hat{V}_1)^2\Psi + \hat{W}_1\Psi + \hat{W}_2\Psi$$

Here $\hat{W}_1$ and $\hat{W}_2$ are washboard operators for junctions 1 and 2, respectively. While this Hamiltonian is correct, it does not provide us with expressions for the conjugate momentum operators; $\hat{p}_1$ and $\hat{p}_2$ can be defined as before, but these are *not* necessarily conjugate to $\hat{\gamma}_1$ and $\hat{\gamma}_2$ for the coupled system!

$$\hat{p}_n \equiv C_J\left(\tfrac{\Phi_0}{2\pi}\right)\hat{V}_n \qquad [\hat{\gamma}_n, \hat{p}_n] = ?$$

In order to find conjugate momentum operators $\hat{p}_n'$, it is helpful to revert to the classical-Lagrangian approach from the method in section 2. The Hamiltonian can be split into a $\hat{W}$ term that depends only on powers of $\hat{\gamma}_1, \hat{\gamma}_2$ and a $\hat{T}$ term that depends only on quadratic combinations of $\hat{V}_1$ and $\hat{V}_2$. Temporarily replacing all quantum operators with their corresponding classical variables, we find:

$$\mathfrak{L} = T - W = \tfrac{1}{2}\left(\tfrac{\Phi_0}{2\pi}\right)^2\left[(C_J + C_C)\dot{\gamma_1}^2 + (C_J + C_C)\dot{\gamma_2}^2 - 2C_C\dot{\gamma_1}\dot{\gamma_2}\right] - W(\gamma_1, \gamma_2)$$

$$p_1' \equiv \tfrac{\partial\mathfrak{L}}{\partial\dot{\gamma_1}} = \left(\tfrac{\Phi_0}{2\pi}\right)^2\left((C_J + C_C)\dot{\gamma_1} - C_C\dot{\gamma_2}\right) = \left(\tfrac{\Phi_0}{2\pi}\right)\left((C_J + C_C)V_1 - C_C V_2\right)$$

and similarly for p_2' . Now the system is "re-quantized" by imposing quantum commutation relations:

$$\hat{p}_1' \equiv \left(\tfrac{\Phi_0}{2\pi}\right)\left((C_J + C_C)\hat{V}_1 - C_C\hat{V}_2\right) \qquad [\hat{\gamma}_1, \hat{p}_1'] = \imath\hbar \qquad \hat{p}_1'\Psi = \imath\hbar\partial_{\gamma_1}\Psi$$

To check that the proposed Hamiltonian is correct, use Heisenberg's equation:

$$\tfrac{d}{dt}\langle\hat{p}_1'\rangle = \tfrac{\imath}{\hbar}\langle[\hat{H}, \hat{p}_1']\rangle = \tfrac{\imath}{\hbar}\langle[\hat{W}_1, \hat{p}_1']\rangle = \left(\tfrac{\Phi_0}{2\pi}\right)\langle I_1 - I_{s1}\rangle$$

$$\tfrac{d}{dt}\langle\hat{p}_1'\rangle = \left(\tfrac{\Phi_0}{2\pi}\right)\left((C_J + C_C)\tfrac{d}{dt}\langle V_1\rangle - C_C\tfrac{d}{dt}\langle V_2\rangle\right)$$

$$C_J\tfrac{d}{dt}\langle V_1\rangle - C_C\tfrac{d}{dt}\langle V_2 - V_1\rangle + \langle I_{s1}\rangle = \langle I_1\rangle$$

Here the correct Kirchhoff's law behavior was found using the rule that partial derivatives commute (thus $[\hat{p}_1', \hat{p}_2'] = 0$), the fact that $\hat{W}_2$ is independent of γ_1 (thus $[\hat{p}_1', \hat{W}_2] = 0$), and Josephson's equations. A similar result for p_2' and the other current-conservation equation can be found by the same methods. The conjugate momentum operators obtained this way have a useful physical interpretation as total charge operators for the left and right nodes between each junction and the coupling capacitor [14].

As the final step, rewrite the Hamiltonian in terms of the "original" momenta $\hat{p}_n$, invert the equations defining $\hat{p}_n'$ for $\hat{p}_n$, and substitute. Define "moment of inertia" and coupling strength as the following:

$$\mu \equiv C_J\left(\tfrac{\Phi_0}{2\pi}\right)^2 \qquad \chi \equiv \tfrac{C_C}{C_J} \qquad \hat{T} = \tfrac{1}{2\mu}\left(\hat{p}_1^2 + \hat{p}_2^2 + \chi(\hat{p}_2 - \hat{p}_1)^2\right)$$

$$\begin{bmatrix} \hat{p}_1' \\ \hat{p}_2' \end{bmatrix} = \begin{bmatrix} 1+\chi & -\chi \\ -\chi & 1+\chi \end{bmatrix}\begin{bmatrix} \hat{p}_1 \\ \hat{p}_2 \end{bmatrix} \Leftrightarrow \begin{bmatrix} \hat{p}_1 \\ \hat{p}_2 \end{bmatrix} = \tfrac{1}{1+2\chi}\begin{bmatrix} 1+\chi & \chi \\ \chi & 1+\chi \end{bmatrix}\begin{bmatrix} \hat{p}_1' \\ \hat{p}_2' \end{bmatrix}$$

Noticing that $\hat{T}$ can itself be written as a < row vector | matrix | column vector > contraction, we find:

$$M \equiv \begin{bmatrix} 1+\chi & -\chi \\ -\chi & 1+\chi \end{bmatrix} \qquad \hat{T} = \frac{1}{2\mu} [\hat{p}_1, \hat{p}_2] \begin{bmatrix} M \end{bmatrix} \begin{bmatrix} \hat{p}_1 \\ \hat{p}_2 \end{bmatrix}$$

Defining "conjugate momentum" and "original momentum" column vectors $\mathfrak{p}$ and $\mathbf{P}$, we can write:

$$\hat{T} = \tfrac{1}{2\mu} \mathbf{p}^T M \mathbf{p} \qquad \mathfrak{p} = M\mathbf{p} \qquad \hat{T} = \tfrac{1}{2\mu}(M^{-1}\mathfrak{p})^T \, M(M^{-1}\mathfrak{p}) = \tfrac{1}{2\mu}\mathfrak{p}^T M^{-1}\mathfrak{p}$$

where we have used the fact that *M* is symmetric. In terms of conjugate momenta, the Hamiltonian is:

$$\hat{H} = \frac{1}{2\mu}\left(\frac{1+\chi}{1+2\chi}\left((\hat{p}_1')^2 + (\hat{p}_2')^2 \right) + \frac{2\chi}{1+2\chi}\left(\hat{p}_1'\hat{p}_2' \right) \right) + \hat{W}_1 + \hat{W}_2$$

Since $[\hat{p}_1', \hat{p}_2'] = 0$ (partial derivatives commute), this Hamiltonian is unchanged by swapping $\hat{p}_1'$ and p_2' . In the wavefunction representation where Ψ is a function of γ_1 and γ_2 , the Schrödinger equation is:

$$\imath\hbar\partial_t \Psi = -\frac{\hbar^2}{2\mu}\left(\frac{1+\chi}{1+2\chi}\left(\partial_{\gamma_1}^2 \Psi + \partial_{\gamma_2}^2 \Psi \right) + \frac{2\chi}{1+2\chi}\left(\frac{\partial^2}{\partial_{\gamma_1}\partial_{\gamma_2}}\Psi \right) \right) + W(\gamma_1)\Psi + W(\gamma_2)\Psi$$

In the next subsection, a generalized version of this method is developed for more complicated systems.

4.2 Multiple junctions connected by capacitors

The following algorithm for finding a multiple-junction Hamiltonian is proposed:

1. Define voltage, junction momentum, and washboard operators for each junction:

$$\hat{V}_n \equiv \left(\tfrac{\Phi_0}{2\pi}\right)\dot{\gamma}_n \qquad \hat{p}_n \equiv C_J\left(\tfrac{\Phi_0}{2\pi}\right)\hat{V}_n \qquad \hat{W}_n \equiv \left(\tfrac{\Phi_0}{2\pi}\right)\left(-I_0\sin(\gamma_n) - I_n\gamma_n\right)$$

2. For each junction, add a "capacitor energy" term and a "washboard energy" term to the Hamiltonian:

$$\hat{H}_n = \tfrac{1}{2}C_J\hat{V}_n^2 + \hat{W}_n = \tfrac{1}{2\mu}\,\hat{p}_n^2 + \hat{W}_n \qquad \mu \equiv C_J\left(\tfrac{\Phi_0}{2\pi}\right)^2$$

3. For any capacitor connected between junctions ℓ and *m* , add another "capacitor energy" term:

$$\hat{H}_{lm} = \tfrac{1}{2}C_C(\hat{V}_l - \hat{V}_m)^2 = \tfrac{1}{2\mu}\,\chi\,(\hat{p}_l - \hat{p}_m)^2 \qquad \chi \equiv \tfrac{C_C}{C_J}$$

The complete Hamiltonian is found by simply adding all of these terms. Each junction momentum operator $\hat{p}_n$ is *not* necessarily conjugate to $\hat{\gamma}_n$, however; the conjugate momentum operators $\hat{p}'_n$ will be linear combinations of the junction momenta $\hat{p}_n$. To see this, note that the Hamiltonian is the sum of a $\hat{W}$ term which depends only on $\gamma_1, \gamma_2, \cdots$ and a $\hat{T}$ term which is a quadratic form of the operators $\hat{p}_n$:

$$
\hat{T} = \frac{1}{2} [\hat{V}_1, \hat{V}_2, \cdots]
\begin{bmatrix}
C_{11} & C_{12} & \cdots \\
C_{21} & C_{22} & \cdots \\
\vdots & \vdots & \ddots
\end{bmatrix}
\begin{bmatrix}
\hat{V}_1 \\
\hat{V}_2 \\
\vdots
\end{bmatrix}
$$

The terms C_{ij} of this capacitance matrix can be found from the Laplacian matrix[5] $\mathcal{L}$ of the circuit:

$$
\mathcal{L}_{ij} \equiv
\begin{cases}
\text{degree}(j) & \text{if } i = j \\
-1 & \text{if junction } i \text{ is connected to junction } j \\
0 & \text{if } i \neq j \text{ and } i \text{ is not connected to } j
\end{cases}
$$

where degree(*j*) is the number of junctions connected to junction number *j*. The capacitance matrix is:

$$
C_{ij} = C_J \, \delta_{ij} + C_C \, \mathcal{L}_{ij}
$$

The $\hat{T}$ operator can be rewritten in terms of junction momenta $\hat{p}_n$ by simply rearranging constants:

$$
\hat{T} = \frac{1}{2} \, C_J^{-2} \left(\frac{\Phi_0}{2\pi} \right)^{-2} \mathbf{p}^T [C] \mathbf{p} = \frac{1}{2\mu} \mathbf{p}^T [M] \mathbf{p} \qquad M_{ij} \equiv C_{ij} \, / \, C_J
$$

The matrix *M* relates the conjugate momenta $\mathfrak{p}$ to the junction momenta $\mathbf{p}$. Once again reverting to the classical Lagrangian in which γ and $\dot{\gamma}$ are treated as coordinates and $p_n = \mu \dot{\gamma}_n$, we find:

$$
p'_j \equiv \frac{\partial \mathcal{L}}{\partial \dot{\gamma}_j} = \frac{\partial T}{\partial \dot{\gamma}_j} = \frac{1}{2\mu} \frac{\partial}{\partial \dot{\gamma}_j} \left(\mathbf{p}^T [M] \mathbf{p} \right) = \frac{\mu}{2} \frac{\partial}{\partial \dot{\gamma}_j} \sum_{i=1}^{N} \sum_{j=1}^{N} \dot{\gamma}_i M_{ij} \dot{\gamma}_j
$$

The double-sum includes diagonal terms $M_{jj} \dot{\gamma}_j^2$ and off-diagonal terms $M_{ij} \dot{\gamma}_i \dot{\gamma}_j + M_{ji} \dot{\gamma}_j \dot{\gamma}_i$, thus

$$
p'_j = \mu \sum_{i=1}^{N} M_{ij} \dot{\gamma}_i = [M] \mathbf{p}_j \quad \Rightarrow \quad \mathfrak{p} = [M] \mathbf{p}
$$

---

[5] Not to be confused with the Lagrangian $\mathcal{L}$, the Laplacian operator ∇^2, or angular momentum *L* !

As with the 2-junction system, we can invert M and substitute into $\hat{T}$ to find $\hat{H}$ in terms of the phase operators $\hat{\gamma}_n$ and their conjugate momentum operators $\hat{p}'_n$. The complete formula for $\hat{H}$ is thus:

$$\mathfrak{p} \equiv [\hat{p}'_1, \hat{p}'_2, \cdots]^T \qquad M_{ij} \equiv \delta_{ij} + \chi\, \mathcal{L}_{ij} \qquad \chi \equiv \frac{C_C}{C_J} \qquad \mu \equiv C_J \left(\frac{\Phi_0}{2\pi}\right)^2$$

$$\hat{H} = \hat{T} + \hat{W} = \frac{1}{2\mu}\left(\mathfrak{p}^T M^{-1} \mathfrak{p}\right) + \hat{W}_1 + \hat{W}_2 + \cdots$$

In the wavefunction representation where Ψ is a function of $\gamma_1, \gamma_2, \ldots$, the Schrödinger equation is:

$$\imath\hbar\partial_t = -\frac{\hbar^2}{2\mu}[\partial_{\gamma_1}, \partial_{\gamma_2}, \cdots] \left[\quad M^{-1} \quad\right] \begin{bmatrix} \partial_{\gamma_1} \\ \partial_{\gamma_2} \\ \vdots \end{bmatrix} + W(\gamma_1) + W(\gamma_2) + \cdots$$

The conjugate momentum operators, Hamiltonian operator, and Schrödinger equation can thus be constructed for any system of identical junctions coupled by identical capacitors (in the limit $R \to \infty$) from knowing only $C_J, C_C, I_0, \{I_n\}$ and the Laplacian matrix $\mathcal{L}$ of the circuit diagram.

The circuit diagram for a multiple-junction system can be simplified with a basic result from graph theory: the Laplacian matrix for a system of capacitively-coupled junctions can be uniquely represented by a (finite, simple, undirected) graph. Each vertex represents a Josephson junction (including both its intrinsic capacitance and tunneling channel), and each edge represents a capacitor between two junctions. For example, the 2-junction system can be represented in the following way:
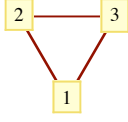
$$\boxed{2}\rule{2cm}{0.4pt}\boxed{1} \qquad\qquad \mathcal{L} = \begin{bmatrix} 2 & -1 \\ -1 & 2 \end{bmatrix} \qquad M = \begin{bmatrix} 1 + 2\chi & -\chi \\ -1\chi & 1 + 2\chi \end{bmatrix}$$

A circuit graph thus provides all the information necessary to construct $\mathcal{L}$. Including the capacitance values, critical current, and bias currents $C_J, C_C, I_0, \{I_n\}$ provides enough information to construct $\hat{H}$. Examples of all possible inequivalent circuit diagrams with 4 or fewer junctions are shown in Appendix C.

Unfortunately, the Schrödinger equation will in general be a system of coupled nonlinear second-order partial differential equations. There are, however, features about the system which can be determined without solving or even approximating the Schrödinger equation. In particular, the possible degeneracies (if any) of any metastable states of the system can be determined by the symmetries of the Hamiltonian. If all bias currents are equal, the washboard operator $\hat{W}_1 + \hat{W}_2 + \cdots$ will be symmetric under any permutation of junction indices. Any such permutation that leaves $\hat{T}$ invariant is thus a symmetry of $\hat{H}$.

4.3 Symmetric systems of coupled junctions

Consider the maximally-connected system of three identical junctions with identical capacitors:

$$\mathcal{L} = \begin{bmatrix} 2 & -1 & -1 \\ -1 & 2 & -1 \\ -1 & -1 & 2 \end{bmatrix} \qquad M = \begin{bmatrix} 1+2\chi & -\chi & -\chi \\ -\chi & 1+2\chi & -\chi \\ -\chi & -\chi & 1+2\chi \end{bmatrix}$$

Any permutation of these three indices leaves the graph unchanged. The permutations of any three objects form a group S_3. These permutations can be represented by matrices which act on $\gamma_1, \gamma_2, \gamma_3$:

$$R_{123} = \begin{bmatrix} 1 & 0 & 0 \\ 0 & 1 & 0 \\ 0 & 0 & 1 \end{bmatrix} \qquad R_{231} = \begin{bmatrix} 0 & 0 & 1 \\ 1 & 0 & 0 \\ 0 & 1 & 0 \end{bmatrix} \qquad R_{312} = \begin{bmatrix} 0 & 1 & 0 \\ 0 & 0 & 1 \\ 1 & 0 & 0 \end{bmatrix}$$

$$R_{213} = \begin{bmatrix} 0 & 1 & 0 \\ 1 & 0 & 0 \\ 0 & 0 & 1 \end{bmatrix} \qquad R_{132} = \begin{bmatrix} 1 & 0 & 0 \\ 0 & 0 & 1 \\ 0 & 1 & 0 \end{bmatrix} \qquad R_{321} = \begin{bmatrix} 0 & 0 & 1 \\ 0 & 1 & 0 \\ 1 & 0 & 0 \end{bmatrix}$$

The total washboard operator $\hat{W} = \hat{W}_1 + \hat{W}_2 + \hat{W}_3$ is unchanged by any permutation of indices. An S_3 permutation does not change the system graph, so it does not change $\mathcal{L}$. $\hat{T}$ is found using only $\mathcal{L}$ and several system constants, so S_3 permutations must not change $\hat{T}$. More precisely, consider any transformation R acting on $\mathbf{P}$. Let $\hat{T}_R$ denote the new $\hat{T}$ operator resulting from this transformation:

$$\hat{T} = \tfrac{1}{2\mu}\mathbf{p}^T M \mathbf{p} \qquad \hat{T}_R \equiv \tfrac{1}{2\mu}(R\mathbf{p})^T M(R\mathbf{p}) = \tfrac{1}{2\mu}\mathbf{p}(R^T M R)\mathbf{p}$$

It follows that the $\hat{T}$ operator is unchanged if and only if $M = R^T M R$. If R is orthogonal, then

$$R^T M R = R^T(1 + \chi\mathcal{L})R = R^T R + \chi R^T \mathcal{L} R = 1 + \chi R^T \mathcal{L} R$$

so if $\mathcal{L} = R^T \mathcal{L} R$ and R is orthogonal, then acting R on $\mathbf{P}$ leaves $\hat{T}$ unchanged. Permutation matrices are orthogonal, so any permutation that commutes with $\mathcal{L}$ must leave $\hat{T}$ (and thus $\hat{H}$) unchanged.

It may be helpful to work through an explicit example. Act the permutation matrix R_{231} on $\mathbf{P}$ to find:

$$\mathbf{P}_R = \begin{bmatrix} \hat{p}_2 \\ \hat{p}_3 \\ \hat{p}_1 \end{bmatrix} \qquad \hat{T}_R = \frac{1}{2\mu}[\hat{p}_2, \hat{p}_3, \hat{p}_1] \begin{bmatrix} 1+2\chi & -\chi & -\chi \\ -\chi & 1+2\chi & -\chi \\ -\chi & -\chi & 1+2\chi \end{bmatrix} \begin{bmatrix} \hat{p}_2 \\ \hat{p}_3 \\ \hat{p}_1 \end{bmatrix}$$

$$= \frac{1}{2\mu}[\hat{p}_2, \hat{p}_3, \hat{p}_1] \begin{bmatrix} (1+2\chi)\hat{p}_2 - \chi\hat{p}_3 - \chi\hat{p}_1 \\ -\chi\hat{p}_2 + (1+2\chi)\hat{p}_3 - \chi\hat{p}_1 \\ -\chi\hat{p}_2 - \chi\hat{p}_3 + (1+2\chi)\hat{p}_1 \end{bmatrix} = \frac{1}{2\mu}[\hat{p}_1, \hat{p}_2, \hat{p}_3] \begin{bmatrix} (1+2\chi)\hat{p}_1 - \chi\hat{p}_2 - \chi\hat{p}_3 \\ -\chi\hat{p}_1 + (1+2\chi)\hat{p}_2 - \chi\hat{p}_3 \\ -\chi\hat{p}_1 - \chi\hat{p}_2 + (1+2\chi)\hat{p}_3 \end{bmatrix} = \frac{1}{2\mu}\mathbf{p}^T M \mathbf{p}$$

In this particular example, any S_3 permutation leaves $\hat{T}$ unchanged. For a general system of N junctions, only some permutations in S_N will be symmetries of $\hat{T}$. These permutations will form a subgroup of S_N .

It is helpful at this point to introduce two definitions from group theory, both using the term "invariant." Let a symmetry group *G* be represented by transformations { R_g } on the vector space $(\gamma_1, \gamma_2, \cdots)$.

1. If $\mathcal{L} = R^T \mathcal{L} R$, then $\mathcal{L}$ is said to be *invariant* under *R,* and *R* represents a symmetry of $\mathcal{L}$.

2. A *G-invariant subspace* is a subspace *V* for which $R_g \mathbf{v} \in V$ for any **v** in *V* and any R_g representing an element of *G.* (Vectors cannot "leave" an *G*-invariant subspace by means of an R_g transformation.)

If $\mathcal{L}$ is invariant under a permutation representation R_g , then $\hat{H}$ must also be invariant under R_g . If *V* is *G*-invariant, then all the vectors in *V* will have the same energy eigenvalues, as shown below.

Let distinct energy eigenstates Ψ_1, Ψ_2 be related to each other by an orthogonal transformation *R* which represents a symmetry of $\hat{H}$. Those two states must have the same energy eigenvalue:

$$\hat{H} = R^T \hat{H} R \quad \text{and} \quad \hat{H}\Psi_1 = E_1\Psi_1 \quad \text{and} \quad R\Psi_1 = \Psi_2$$
$$\Rightarrow E_1\Psi_1 = \hat{H}\Psi_1 = (R^T\hat{H}R)\Psi_1 = R^T\hat{H}\Psi_2 = E_2 R^T \Psi_2 = E_2\Psi_1 \Rightarrow E_2 = E_1$$

If these two states are linearly independent, they are said to be *degenerate*. (Any linear combination of Ψ_1, Ψ_2 will also have the same energy eigenvalue; hence the restriction of linear independence.) Therefore if { R_g } has an invariant subspace of dimension *d* , it is possible to construct *d* linearly independent eigenstates with the same energy eigenvalue. $\hat{H}$ is then said to have a *d-degeneracy.*

For a Hamiltonian $\hat{H}$ with a symmetry group *G*, the following algorithm can be used to find degeneracies:

1. Find the dimensions of the invariant subspaces of the orthogonal representations of *G*.

Each invariant subspace of dimension *d* corresponds to a *d*-degeneracy of $\hat{H}$. The invariant subspace dimensions for N-degree representations of the symmetry groups of 3- and 4-junction systems are listed in Appendix C; these are the degeneracies for the singly-excited states of each system. For the sake of clarity, examples for S_3 are worked out explicitly on the following page. We start with the permutation-matrix representation of S_3 and show that invariant subspaces of dimension 1 and 2 exist [24]. Consider the action of the permutation matrices *R* on the following orthogonal basis elements:

$$\mathbf{b}_1 = [1, 1, 1]^T \qquad \mathbf{b}_2 = [1, 0, -1]^T \qquad \mathbf{b}_3 = [1, -2, 1]^T$$

Any permutation of the components of $\mathbf{b}_1$ will obviously leave $\mathbf{b}_1$ unchanged; what about the other two?

$$[R_{231}]\mathbf{b}_2 = \begin{bmatrix} 0 \\ -1 \\ 1 \end{bmatrix} = -\frac{1}{2}\mathbf{b}_2 + \frac{1}{2}\mathbf{b}_3 \qquad [R_{231}]\mathbf{b}_3 = \begin{bmatrix} -2 \\ 1 \\ 1 \end{bmatrix} = -\frac{3}{2}\mathbf{b}_2 - \frac{1}{2}\mathbf{b}_3$$

$$[R_{213}]\mathbf{b}_2 = \begin{bmatrix} 0 \\ 1 \\ -1 \end{bmatrix} = \frac{1}{2}\mathbf{b}_2 - \frac{1}{2}\mathbf{b}_3 \qquad [R_{213}]\mathbf{b}_3 = \begin{bmatrix} -2 \\ 1 \\ 1 \end{bmatrix} = -\frac{3}{2}\mathbf{b}_2 - \frac{1}{2}\mathbf{b}_3$$

$$[R_{312}]\mathbf{b}_2 = \begin{bmatrix} -1 \\ 1 \\ 0 \end{bmatrix} = -\frac{1}{2}\mathbf{b}_2 - \frac{1}{2}\mathbf{b}_3 \qquad [R_{312}]\mathbf{b}_3 = \begin{bmatrix} 1 \\ 1 \\ -2 \end{bmatrix} = \frac{3}{2}\mathbf{b}_2 - \frac{1}{2}\mathbf{b}_3$$

and so on for R_{132} and R_{321} . In every case, acting R on $\mathbf{b}_2$ or $\mathbf{b}_3$ produces a vector that is a linear combination of $\mathbf{b}_2$ and $\mathbf{b}_3$, so $\mathbf{b}_2$ and $\mathbf{b}_3$ form a basis for an invariant subspace of the R matrices.

The R matrices have invariant subspace dimensions {1,2}, so the first excited state of the "triangle-junction" system has degeneracies {1,2}. This can be seen by using the direct products of metastable single-junction states as a basis for multiple-junction excited states. Represent the state "junction 1 and 2 are in their ground states and junction 3 is in its first-excited state" by the vector |001>, and so on. Consider the following choice of basis for a singly-excited system:

$$\Psi_a = \frac{1}{\sqrt{3}}(|100\rangle + |010\rangle + |001\rangle) \qquad \Psi_b = \frac{1}{\sqrt{2}}(|100\rangle - |001\rangle) \qquad \Psi_c = \frac{1}{\sqrt{6}}(|100\rangle - 2|010\rangle + |001\rangle)$$

Any 3-permutation applied to Ψ_a leaves Ψ_a unchanged and any such permutation applied to a linear combination of Ψ_b and Ψ_c will produce another linear combination of Ψ_b and Ψ_c . Since every 3-permutation is a symmetry of $\hat{H}$, it follows that any linear combination of Ψ_b and Ψ_c must share the same energy eigenvalue as any other linear combination of Ψ_b and Ψ_c . Therefore, the singly-excited states of the triangle-junction system can be partitioned into a single state Ψ_a plus a doubly-degenerate eigenspace equal to the span of Ψ_b and Ψ_c .

For the triangle-junction system, any 3-permutation is a symmetry of the system. For a general N-junction system, the permutation symmetries of $\hat{H}$ will form a subgroup of S_N and degenerate states will form an invariant subspace of a representation of that subgroup. A maximally-connected N-junction system will have singly-excited degeneracies {1, N-1} because the invariant subspaces of an N-degree representation of S_N have dimensions {1, N-1}. Any junction system with an Abelian symmetry group will have no degeneracy because Abelian group representations are always completely reducible [24].

5.   Proposals for future research

Systems of Josephson junctions are useful for the construction of phase-qubit based quantum computers and are of theoretical interest as examples of macroscopic quantum entanglement. In addition, the ability to alter junction energies and couplings makes multiply-coupled systems attractive as models of molecular behavior, and much of the relevant mathematics applies to molecular chemistry as well as junction physics. With these applications in mind, the study of degenerate systems of junctions presented in this paper is intended as a preliminary exercise towards a larger goal: approximating the time evolution of an arbitrary system of junctions subject to time-dependent bias currents.

The first step towards this goal, which is to write the Schrödinger equation for an arbitrary system, has been accomplished. Another useful step is to write system states in terms of the direct-product basis formed by single-junction states, which is the motivation for introducing the group-theoretical methods of section 4. Because the single-junction Schrödinger equation can be numerically analyzed more easily than a multiple-junction equation, these direct-product states can be approximated relatively easily.

Several more proposals for future research into Josephson junction system behavior are listed below.

1. Extend the methods here to multiply-excited systems. If m energy quanta are distributed among N junctions, the direct-product basis will consist of Multiset(N,m) states[6]. Finding the degenerate states of such a system requires finding a unitary irrep of degree Multiset(N,m) for the system symmetry group.

2. Consider possible symmetries that are *not* permutations. For example, the washboard potential is often approximated as locally quadratic near a local minimum for metastable states. A sum of identical quadratic potentials can be written as a diagonal quadratic form, and symmetries of $\hat{T}$ that are not permutation symmetries may be approximate symmetries of $\hat{H}$ if $\hat{W}$ is approximately quadratic.

3. Estimate the effects of small-scale symmetry-breaking. No junctions or capacitors are ever *exactly* identical, and thus the degeneracies derived here are expected to be approximate. Avoided-crossing behavior is expected for imperfectly degenerate systems, and the energy gap between crossings is expected to increase if any junctions are detuned by error or by deliberate application of bias current.

5. Attempt to model environmental interactions, nonzero temperature effects, and/or barrier impurities. Possible strategies include random matrices representing unknown interactions, "heat bath" Hamiltonians of many harmonic oscillators, and transfer-matrix scattering models of barrier imperfections. Are multiple-junction entanglements more stable against such effects? If so, can those systems be used as qubits?

6. Experimentally test predicted degeneracies and the voltage-supercurrent uncertainty relationship. The former can be tested by spectroscopy experiments; the author welcomes suggestions for the latter!

––––––––––––––––––––

[6] Multiset(N,m) is the multiset coefficient $\binom{N+m-1}{m} = \frac{(N+m-1)!}{m!(N-1)!}$ familiar from statistical physics.

Bibliography

[1] Brian D. Josephson **Possible New Effects in Superconductive Tunneling** Phys. Lett. 1, 251 (1962)

[2] Donald G. McDonald **The Nobel Laureate Versus the Graduate Student** Physics Today, July (2001)

[3] Richard Feynman, Robert B. Leighton, Matthew Sands: **The Feynman Lectures on Physics Vol. 3** Pearson/Addison/Wesley (1963)

[4] Werner Buckel, Reinhold Kleiner **Superconductivity: Fundamentals and Applications** Wiley-VCH (2004)

[5] Steven H. Strogatz **Nonlinear Dynamics and Chaos** Westview (2000)

[6] Yakir Aharonov, Daniel Rohrlich **Quantum Paradoxes: Quantum Theory for the Perplexed** Wiley-VCH (2005)

[7] David J. Griffiths **Introduction to Quantum Mechanics** Prentice Hall (1995)

[8] Robert Gilmore **Elementary Quantum Mechanics in One Dimension** Johns Hopkins Univ. Press (2004)

[9] Robert Gilmore **Lie Groups, Physics, and Geometry** Cambridge (2008)

[10] Leslie E. Ballentine **Quantum Mechanics: A Modern Development** World Scientific (2006)

[11] Stephen H. Friedberg, Arnold J. Insel, Lawrence E. Spence **Linear Algebra** (3rd Ed.) Prentice Hall (1997)

[12] C. H. Edwards Jr, David E. Penney **Differential Equations and Boundary Value Problems** Prentice Hall (1996)

[13] Timothy Jones **Is Quantum Decoherence the Von Neumann Wave Collapse?** Ph.D qualifying exam, Drexel University (2006)

[14] Zechariah E. Thrailkill **Spectroscopy of Multiple Coupled Josephson Phase Qubits** Ph.D qualifying exam, Drexel University (2007)

[15] Philip R. Johnson, Frederick W. Strauch, Alex J. Dragt, Roberto C. Ramos, C. J. Lobb, J. R. Anderson, F. C. Wellstood **Spectroscopy of Capacitively Coupled Josephson-junction Qubits** Physical Review B 67 (2003)

[16] Erica Caden, Robert Gilmore **Quantum Mechanical Reflection Resonances** arXiv (2008)

[17] Frederick W. Strauch **Theory of Superconducting Phase Qubits** Ph.D thesis, University of Maryland - College Park (2004)

[18] Herbert Goldstein, Charles Poole, John Safko **Classical Mechanics** 3rd Ed. Addison Wesley (2002)

[19] A. J. Berkley, H. Xu, M. A. Gubrud, R. C. Ramos, J. R. Anderson, C. J. Lobb, F. C. Wellstood **Decoherence in a Josephson-junction Qubit** Phys. Rev. B 68 (2003)

[20] Huizhong Xu **Quantum Computing with Josephson Junction Circuits**, Ph.D. thesis, University of Maryland-College Park (2004)

[21] Roger Penrose **The Road to Reality: A Complete Guide to the Laws of the Universe.** Random House (2004)

[22] M. H. Devoret, A. Wallraff, J. M. Martinis **Superconducting Qubits: A Short Review** arXiv (2004)

[23] K. Dukhatme, Y. Mukharsky, T. Chui, D. Pearson **Observation of the Ideal Josephson Effect in Superfluid ^{4}He** Nature 411 (2001)

[24] Peter Szekeres **A Course In Modern Mathematical Physics: Groups, Hilbert Space, and Differential Geometry** Cambridge (2004)

[25] A. J. Berkley, H. Xu, R. C. Ramos, M. A. Gubrud, F. W. Strauch, P. R. Johnson, J. R. Anderson, A. J. Dragt, C. J. Lobb, F. C. Wellstood **Entangled Macroscopic Quantum States in Two Superconducting Qubits** Science 300 (2003)

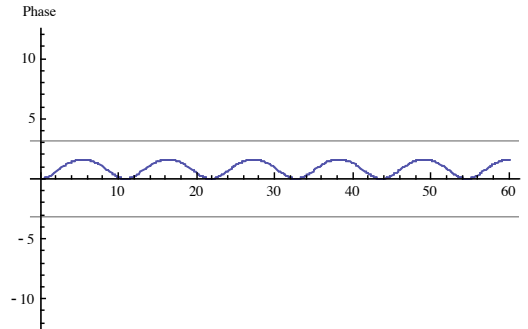## Appendix A: Numerical results for classical pendulum equation of motion

Approximate solutions for the classical 360° pendulum with constant torque Γ were found for various initial conditions using Mathematica. The code used is displayed below with some sample results.

Equation of motion: $\gamma''(t) = \Gamma/(m\ r^2)- g/r \cos(\gamma(t))$
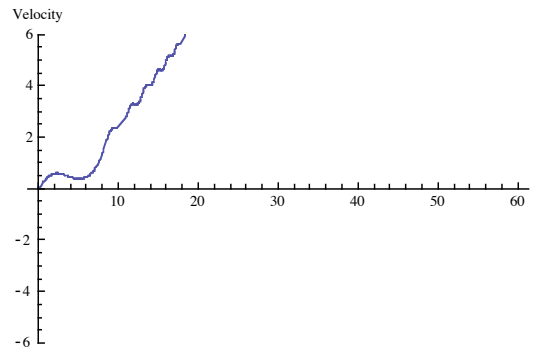Example constants: m = 100 Kg , r = 3 m , g = 1.6 m/s²

Phase coordinate γ(t)
Manipulate[Plot[Evaluate[{γ[t]}/.NDSolve[{γ''[t] == Γ/900- 1.6/3 Sin[γ[t]], γ[0]==0, γ'[0]==0}, γ, {t,0,60}]], {t, 0,60},PlotRange->{-4 π,4 π}, GridLines->{{0},{-π, 0, π}},AxesLabel->{t,Phase}], {Γ,0,500}]

Phase velocity γ'(t)
Manipulate[Plot[Evaluate[{γ'[t]}/.NDSolve[{γ''[t] == Γ/900- 1.6/3 Sin[γ[t]], γ[0]==0, γ'[0]==0}, γ, {t,0,60}]], {t, 0,60}, PlotRange->{-6,6},AxesLabel->{t,Velocity}], {Γ,0,500}]

Binding energy 1/2 m r^2 [γ' (t)]²- m g r cos[γ(t)] - m g r
(kinetic energy + gravitational potential energy - energy needed to reach γ = π)
Manipulate[Plot[Evaluate[{1/2 900 (γ'[t])²-100*1.6*3*Cos[γ[t]]-100*1.6*3}/.NDSolve[{γ''[t] == Γ/900- 1.6/3 Sin[γ[t]], γ[0]==0, γ'[0]==0}, γ, {t,0,60}]], {t,0,60}, PlotRange->{-960,300},AxesLabel->{t,Binding Energy}, GridLines->{{0},{-960,0}}], {Γ,0,500}]
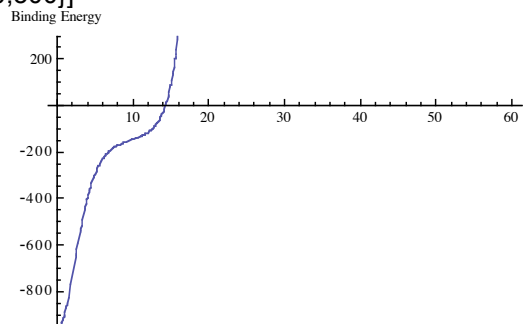
Appendix B: Numerical results for single junction with hard-wall boundary conditions

As an example of a realistic Josephson junction, the following data were taken from [25]:

$$C_J \approx 4.8 \text{ pF} \qquad I_0 \approx 14.779 \ \mu\text{A} \qquad I_b \approx 14.630 \ \mu\text{A} \approx 0.99 \ I_0$$

Single-junction Hamiltonian:

$$\hat{H}\Psi = \frac{-\hbar^2}{2\mu}\partial_\gamma^2\Psi - \left(\frac{\Phi_0}{2\pi}\right)I_0\cos(\gamma)\Psi - \left(\frac{\Phi_0}{2\pi}\right)I_b\gamma\Psi \qquad \mu \equiv C_J\left(\frac{\Phi_0}{2\pi}\right)^2$$

$$\partial_\gamma^2\Psi = \frac{2\mu}{\hbar^2}\left(\frac{\Phi_0}{2\pi}\right)\left(-I_0\cos(\gamma)\Psi - I_b\gamma\Psi\right)$$

Numerical values of constants:

$$\left(\frac{\Phi_0}{2\pi}\right) \approx 3.291\cdot10^{-16} \text{ V·s} \qquad \mu \approx 5.199\cdot10^{-43} \text{ J·s}^2 \qquad \frac{\hbar^2}{2\mu} \approx 1.070\cdot10^{-26} \text{ J}$$

Local minima and maxima of washboard potential:

$$I_0\sin(\gamma) - I_b = 0 \ \Rightarrow \ \gamma \approx \{\cdots, 1.429, 1.713, \cdots\}$$

Tunneling energy barrier at local maximum $\gamma = 1.713$:

$$W(1.713) = \left(\frac{\Phi_0}{2\pi}\right)\left(-I_0\cos(1.713) - I_b(1.713)\right) \approx -8.94\cdot10^{-21}\text{J}$$

States with energy less than -8.94 10^{-21} J were considered bound; other results were disregarded. By this criteria, four bound states exist with the following binding energies (relative to tunneling barrier):

ground: -7.96371e-24   1st: -5.37347e-24   2nd: -2.94145e-24   3rd: -6.69305e-25

C++ code is attached below:

```
#include<iostream>
#include<fstream>
#include<cstdio>
#include<cstdlib>
#include<cmath>
#include<ctime>
#include<iomanip>
#include<cfloat>

using namespace std;

#include "nrutil.h"
#include "nrutil.c"
#include "nr.h"
#include "Dtqli.c"
```

```c
#include "Dpythag.c"
#include "Deigsrt.c"

#define Pi 3.14159265
#define xval (leftend+(j-1)*delta)

/* POTENTIAL TO BE EVALUATED GOES HERE.  Input a formula for (2m/hbar^2) * V(x). */

double potential(double x){
  double V = - 455045.0*cos(x) -450458.0*x;
  return V;
}

/* Main program*/

main(){

  int N;
  int eigmax;
  double leftend, rightend;
  char flipquestion;
  bool flip;
  double xright, xleft;

/* Input interval length and number of blocks from user.  Block size will be calculated and displayed
      automatically. */

  cout << "\n" << "Left endpoint? ";
  cin >> leftend;
  cout << "Right endpoint? ";
  cin >> rightend;
  cout << "Number of blocks? ";
  cin >> N;
  cout << "Number of eigenvalues and eigenfunctions to store? ";
  cin >> eigmax;
  cout << "Demand positive eigenfunctions for large x?  (Y or N) ";
  cin >> flipquestion;

  if (flipquestion=='Y'){ flip = true; }
  else if (flipquestion=='y'){ flip = true; }
  else { flip = false; }

  double delta = ( rightend - leftend ) / N;
  double deltasqr = delta * delta;
  double invdelta = 1.0 / delta;
  double indsqrd = 1.0 / deltasqr;
  double indsqrt = sqrt(invdelta);

  cout << "\n" << "Block size is " << delta << "\n";

/* Allocate memory for vectors and matrices.  */

  double* diagonal = dvector(1,N);
  double* subdiagonal = dvector(1,N);
  double** Identity = dmatrix(1,N,1,N);

/* Initialize the identity matrix */
```

```cpp
    for(int i=1; i<=N; i++){
      for(int j=1; j<=N; j++){
        if(i==j){ Identity[i][j] = 1.0; } else{ Identity[i][j] = 0; };
      }
    }


    /* Initialize the diagonal and subdiagonal elements of the Hamiltonian matrix. */

    for(int j=1; j<=N; j++){
      diagonal[j] = 1.0 + deltasqr * potential(leftend+(j-1)*delta);
    }

    for(int j=1; j<=N; j++){
      subdiagonal[j] = -0.5;
    }


    /* Call the NR routine "tqli" to diagonalize our Hamiltonian.  Note that [diagonal] will be overwritten
       with UNORDERED energy eigenvalues, [subdiagonal] will be destroyed, and [Identity] will be overwritten
       with column eigenvectors of our Hamiltonian operator. */

    tqli(diagonal, subdiagonal, N, Identity);


    /* Call the NR routine "eigsrt" to sort our eigenvalues and eigenvectors in descending order. */

    eigsrt(diagonal, Identity, N);


    /* Display the lowest energy eigenvalues. */

    cout << "Lowest " << eigmax << " eigenvalues are: \n";

    for(int j = N; j >= N - eigmax + 1 ; j--){
      cout << (indsqrd * diagonal[j] + 707143.0) * 1.070e-26 << "\n";

    /* Eigenvalues have been rescaled specifically for this particular problem !!! */

    }
    cout << "\n" << "\n";


    /* The eigenvectors by "tqli" are normalized using the Pythagorean metric for an N-dimensional Euclidean
       space.  For QM normalizaion, divide all of the components of each eigenvector by sqrt(delta).  */

    for(int j=1; j <=N; j++ ){
      for(int k= N - eigmax+1 ; k <= N ; k++){
        Identity[j][k] = indsqrt * Identity[j][k];
      }
    }

    cout << "Eigenvectors have been normalized as quantum wavefunctions." << "\n";

    /* These eigenvectors are also not necessarily of the same sign as those produced analytically, e.g.
          Hermite polynomials are defined such that the highest power is positive, so the analytic solutions
          will always be positive for large enough x.  The following code attempts to find eigenvectors which
          are negative for large x and flip them upside down.*/
```

```cpp
  if (flip) {
    for(int k = N - eigmax+1 ; k <=N ; k++){

      for(int j = N ; j > 1 ; j-- ){
        if ( fabs(Identity[j][k]) > 0.00001 ){
          if ( Identity[j][k] < 0 ){
            flip = true;
          }
          else { flip = false; }
          j = 1;
        }
      }

      if (flip) {
        for(int j=1; j<=N; j++){
          Identity[j][k] = Identity[j][k] * -1.0;
        }
      }
    }
  }

}


/* Output x-values followed by the last [eigmax] columns of [Identity] to a file.*/

  ofstream schrout;
  schrout.open ("SchroDATA.txt");

  for(int j=1; j <=N; j++ ){
    schrout << xval << "    ";                    // saves x-values
      schrout << (potential( xval ) + 707143.0) * 1.070e-26 << "    ";      // saves potential

      /* Potential output has been rescaled specifically for this particular potential !!! */

    for(int k= N ; k >= N - eigmax + 1 ; k--){
      schrout << Identity[j][k] * 5e-24 << "    ";              // saves column vectors
    }
    schrout << "\n";

      /* Y-axis values for wavefunctions have been rescaled specifically for this particular potential !!! */

  }

  schrout.close();

  cout << "\n * Lowest " << eigmax << " eigenvectors have been saved to SchroDATA.txt * \n\n";


return 0;

}
```

Appendix C: Examples of multiply-coupled Josephson junction systems

3-junction systems:

$$\imath\hbar\partial_t = -\frac{\hbar^2}{2\mu}[\partial_{\gamma_1}, \partial_{\gamma_2}, \partial_{\gamma_3}]\begin{bmatrix} & & \\ & M^{-1} & \\ & & \end{bmatrix}\begin{bmatrix} \partial_{\gamma_1} \\ \partial_{\gamma_2} \\ \partial_{\gamma_3} \end{bmatrix} + W(\gamma_1) + W(\gamma_2) + W(\gamma_3)$$
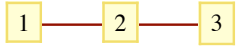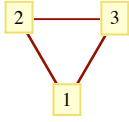

$$\mathcal{L} = \begin{bmatrix} 1 & -1 & 0 \\ -1 & 2 & -1 \\ 0 & -1 & 1 \end{bmatrix} \qquad M = \begin{bmatrix} 1+\chi & -\chi & 0 \\ -\chi & 1+2\chi & -\chi \\ 0 & -\chi & 1+\chi \end{bmatrix}$$

Symmetry group: S_2 Order: 2   Dimension of invariant subspaces: {1,1,1}

$$\mathcal{L} = \begin{bmatrix} 2 & -1 & -1 \\ -1 & 2 & -1 \\ -1 & -1 & 2 \end{bmatrix} \qquad M = \begin{bmatrix} 1+2\chi & -\chi & -\chi \\ -\chi & 1+2\chi & -\chi \\ -\chi & -\chi & 1+2\chi \end{bmatrix}$$

Symmetry group: S_3 Order: 6   Dimension of invariant subspaces: {1, 2}

4-junction systems:

$$\imath\hbar\partial_t = -\frac{\hbar^2}{2\mu}[\partial_{\gamma_1}, \partial_{\gamma_2}, \partial_{\gamma_3}, \partial_{\gamma_4}]\begin{bmatrix} & & \\ & M^{-1} & \\ & & \end{bmatrix}\begin{bmatrix} \partial_{\gamma_1} \\ \partial_{\gamma_2} \\ \partial_{\gamma_3} \\ \partial_{\gamma_4} \end{bmatrix} + W(\gamma_1) + W(\gamma_2) + W(\gamma_3) + W(\gamma_4)$$
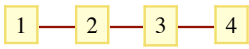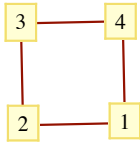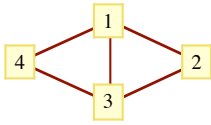

$$\mathcal{L} = \begin{bmatrix} 1 & -1 & 0 & 0 \\ -1 & 2 & -1 & 0 \\ 0 & -1 & 2 & -1 \\ 0 & 0 & -1 & 1 \end{bmatrix} \qquad M = \begin{bmatrix} 1+\chi & -\chi & 0 & 0 \\ -\chi & 1+2\chi & -\chi & 0 \\ 0 & -\chi & 1+2\chi & -\chi \\ 0 & 0 & -\chi & 1+\chi \end{bmatrix}$$

Symmetry group: S_2 Order: 2   Dimension of invariant subspaces: {1,1,1,1}

$$\mathcal{L} = \begin{bmatrix} 2 & -1 & 0 & -1 \\ -1 & 2 & -1 & 0 \\ 0 & -1 & 2 & -1 \\ -1 & 0 & -1 & 2 \end{bmatrix} \qquad M = \begin{bmatrix} 1+2\chi & -\chi & 0 & -\chi \\ -\chi & 1+2\chi & -\chi & 0 \\ 0 & -\chi & 1+2\chi & -\chi \\ -\chi & 0 & -\chi & 1+2\chi \end{bmatrix}$$

Symmetry group: D_4 Order: 8   Dimension of invariant subspaces: {1, 1, 2}
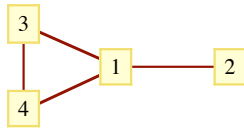

$$\mathcal{L} = \begin{bmatrix} 3 & -1 & -1 & -1 \\ -1 & 2 & -1 & 0 \\ -1 & -1 & 3 & -1 \\ -1 & 0 & -1 & 2 \end{bmatrix} \qquad M = \begin{bmatrix} 1+3\chi & -\chi & -\chi & -\chi \\ -\chi & 1+2\chi & -\chi & 0 \\ -\chi & -\chi & 1+3\chi & -\chi \\ -\chi & 0 & -\chi & 1+2\chi \end{bmatrix}$$

Symmetry group: $S_2 \otimes S_2$ Order: 4   Dimension of invariant subspaces: {1, 1, 1, 1}
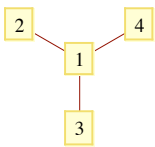

$$\mathcal{L} = \begin{bmatrix} 3 & -1 & -1 & -1 \\ -1 & 1 & 0 & 0 \\ -1 & 0 & 2 & -1 \\ -1 & 0 & -1 & 2 \end{bmatrix} \qquad M = \begin{bmatrix} 1+3\chi & -\chi & -\chi & -\chi \\ -\chi & 1+\chi & 0 & 0 \\ -\chi & 0 & 1+2\chi & -\chi \\ -\chi & 0 & -\chi & 1+2\chi \end{bmatrix}$$

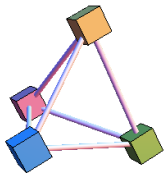Symmetry group: S_2 Order: 2   Dimension of invariant subspaces: {1,1,1,1}

$$\mathcal{L} = \begin{bmatrix} 3 & -1 & -1 & -1 \\ -1 & 1 & 0 & 0 \\ -1 & 0 & 1 & 0 \\ -1 & 0 & 0 & 1 \end{bmatrix} \qquad M = \begin{bmatrix} 1+3\chi & -\chi & -\chi & -\chi \\ -\chi & 1+\chi & 0 & 0 \\ -\chi & 0 & 1+\chi & 0 \\ -\chi & 0 & 0 & 1+\chi \end{bmatrix}$$

Symmetry group: S_3 Order: 6   Dimension of invariant subspaces: {1, 1, 1, 2}

$$\mathcal{L} = \begin{bmatrix} 3 & -1 & -1 & -1 \\ -1 & 3 & -1 & -1 \\ -1 & -1 & 3 & -1 \\ -1 & -1 & -1 & 3 \end{bmatrix} \qquad M = \begin{bmatrix} 1+3\chi & -\chi & -\chi & -\chi \\ -\chi & 1+3\chi & -\chi & -\chi \\ -\chi & -\chi & 1+3\chi & -\chi \\ -\chi & -\chi & -\chi & 1+3\chi \end{bmatrix}$$
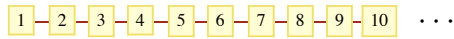
Symmetry group: S_4 Order: 24   Dimension of invariant subspaces: {1, 3}

Some general large-N systems:

Minimally connected "chain" of N junctions

$$\mathcal{L} = \begin{bmatrix} 1 & -1 & 0 & 0 & \cdots \\ -1 & 2 & -1 & 0 & \cdots \\ 0 & -1 & 2 & -1 & \cdots \\ 0 & 0 & -1 & 2 & \cdots \\ \vdots & \vdots & \vdots & \vdots & \ddots \end{bmatrix}$$
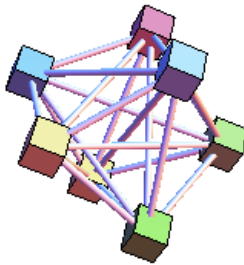

Symmetry group: S_2　　　Order: 2　　　Dimension of invariant subspaces: { 1,1,1,1, ... }

(Any N-junction chain will have S_2 as its symmetry group. Since S_2 is Abelian, no degeneracy exists.)

Maximally connected network of N junctions　　　(example graph shown here for N=7)

$$\mathcal{L} = \begin{bmatrix} (N-1) & -1 & -1 & -1 & \cdots \\ -1 & (N-1) & -1 & -1 & \cdots \\ -1 & -1 & (N-1) & -1 & \cdots \\ -1 & -1 & -1 & (N-1) & \cdots \\ \vdots & \vdots & \vdots & \vdots & \ddots \end{bmatrix}$$
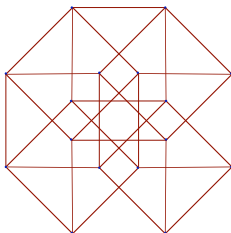
Symmetry group: S_N　　　Order: N !　　　Dimension of invariant subspaces: { 1 , N-1 }

Hypercubic 16-junction system ?

Tesseract (4-cube)

$$\mathcal{L} = \begin{bmatrix} 4 & -1 & 0 & -1 & 0 & 0 & 0 & 0 & \cdots \\ -1 & 4 & -1 & 0 & 0 & 0 & 0 & 0 & \cdots \\ 0 & -1 & 4 & 0 & 0 & -1 & 0 & 0 & \cdots \\ -1 & 0 & 0 & 4 & -1 & 0 & 0 & 0 & \cdots \\ 0 & 0 & 0 & -1 & 4 & 0 & 0 & -1 & \cdots \\ 0 & 0 & -1 & 0 & 0 & 4 & -1 & 0 & \cdots \\ 0 & 0 & 0 & 0 & 0 & -1 & 4 & 0 & \cdots \\ 0 & 0 & 0 & 0 & -1 & 0 & 0 & 4 & \cdots \\ \vdots & \vdots & \vdots & \vdots & \vdots & \vdots & \vdots & \vdots & \ddots \end{bmatrix}$$　?

Symmetry group: C_4　　　Order: 384　　　Dimension of invariant subspaces: { 1, 1, 4, 4, 6 } ?